

Stability and Hopf Bifurcation Analysis of an Infectious Disease Delay Model

IMEKELA D. EZEKIEL^{1,2}, SAMUEL A. IYASE¹, TIMOTHY A. ANAKE¹

¹Department of Mathematics,
Covenant University,
Ota,
NIGERIA

²Department of Mathematics & Statistics,
Federal Polytechnic,
Ilaro,
NIGERIA

Abstract: - This paper investigated the stability of the dynamical behavior of the susceptible (S), infectious (I) and recovered (R) (SIR) disease epidemic model with intracellular time delay that is unable to stabilize the unstable interior non-hyperbolic equilibrium. The study employed characteristics and bifurcation methods for investigating conditions of stability and instability of the SIR disease epidemic model using the dimensionless threshold reproduction value R_0 for the disease-free equilibrium (DFE) point and the endemic equilibrium point. The study confirms that disease-free equilibrium (DFE) point and the endemic equilibrium point cannot coexist simultaneously. The paper equally investigated the local stability analysis of the reduced nonlinear SIR disease epidemic delay model when at least one of the characteristic roots has zero real parts while every other eigenvalue(s) has negative real parts. The result of the analysis of the model showed that the conditions for Hopf bifurcation obtained from the behavior of the systems are sufficient but not necessary since the model is unable to stabilize the unstable interior non-hyperbolic equilibrium. Specifically, the direction of Hopf bifurcation, the stability behavior and the period of the bifurcating periodic solutions of the interior non-hyperbolic equilibrium of the infectious disease model were explicitly determined using methods of the normal form concept (NFC) and the center manifold theorem (CMT) to investigate the transformed reduced operator differential equation (OpDE). The contribution of this paper is based on applications to assess the effectiveness of different control strategies of parameter values for stability properties of infectious disease models and can be found useful to bio-mathematicians, ecologists, biologists and public health workers for decision-making. Finally, a numerical example to verify the analytical finding was performed using the MATLAB software.

Key-Words: - Center Manifold Theorem, Characteristic equation, Hopf bifurcation, Operator differential equation, Stability analysis, Time delay.

Received: August 22, 2024. Revised: December 15, 2024. Accepted: January 8, 2025. Published: March 14, 2025.

1 Introduction

The progression in time of many physical systems is mostly defined through a system of ordinary differential equations (ODEs) which can be rewritten in vector forms. One major challenge in determining realistic results for applications of ODEs to physical systems is that most of these systems hide the effects of time in their occurrences. This challenge provides fewer model parameters and equations, especially in dynamical systems where occurrences are not instantaneous as observed in [1] and [2]. For biological systems involving population systems, infectious disease models

(IDMs), eco-epidemiology models among others, time delays can represent gestation period, incubation period, maturation or generation time and the intracellular delay as found in the works of [3] and [4]. The introduction of this explicit real time delay sometimes captures realistic qualitative dynamics which may require additional variables and parameters that cannot be easily distinguished and determined experimentally by ordinary differential equations (ODEs) as found in [5]. The use of delay differential equations (DDEs) to investigate dynamical behavior of ordinary differential systems (ODSs) provide opportunity where multiple steps within delay models can be

simplified into a single step as in the works of [6] and [7]. In as much as ODEs require exponential solutions to compute the characteristic polynomial function for the characteristic roots, DDEs require exponential solutions to compute the resulting characteristic equation in the form of transcendental function. This makes assumptions and computation of solutions of DDEs different, difficult and complicated to handle. For instance, the occurrences and control of infectious diseases (IDs) on human health over the years is alarming and fast attracting the attention of mathematicians. This, in quest for application calls for mathematical results from epidemiological models that are widely expressed in differential equations (DEs). Some of such infectious disease models include haemorrhagic fever (HF), acute respiratory syndrome (ARS), the popular corona virus (Covid-19), tuberculosis, malaria, cholera among others as found in [7]. For effective control strategies, it is important for individual members of the society to recognize and identify the transmission routes, infection rate, recovery rate and fatality rate among other indices of epidemics in an emerging infectious disease model. Many factors are responsible for the causes, spread and transmission of infectious diseases which are often expressed in mathematical terms as seen in [8] and [9]. The knowledge of transmission processes and epidemics indices provide necessary information that can help individuals to keep away from infected person(s), avoid crowded areas and even shares greater popularity as discussed in [10], [11] and [12]. Also, the progression of infectious disease systems require time to manifest. The need to incorporate delay time in epidemic infectious models make investigation of the qualitative properties of delay systems necessary and more realistic as observed in [4] and [7]. The classification, investigation and analysis of such models is necessary. In this case, the entire population is categorized into different compartment with regards to infection status of the individual or species for stability analysis. One of such classifications into groups is the susceptible group (S), the infected group (I) and the recovered group (R). This classification is popularly called the SIR model and is pioneered by [13]. These classifications fall within the consideration of this paper as observed in [14]. Among the qualitative properties of epidemic models, stability analysis stands out and is widely applied to real life processes in different fields of specializations and of various classifications. These specializations include biology, physics, economics, public health and engineering models among others. The study of

systems with delay, therefore, involves linear and non-linear systems with inherent interactions among models that are being described by a set of differential equations (DEs).

Thus, the investigation of stability analysis of delay systems provides realistic background upon which mathematical models can thrive. For epidemiological systems, the dynamics of infectious diseases model have always attracted the attention of mathematicians to model, control and proffer solutions to outbreak of infectious diseases. The application of mathematics to investigate stability of such infectious disease transmission models have proven very successful, especially during Covid 19 as seen in [15], [16] and [17]. For different forms of infectious disease models, [18]. It is also observed that transmission of infectious diseases are not instantaneous and the inclusion of intracellular finite time delay to investigating the stability of disease transmission model is necessary. This is the aim of this paper. Previous studies opened many deterministic and stochastic models for stability analysis and Hopf bifurcation of nonlinear analysis to investigate qualitative properties of variety of infectious disease models but without delay as seen in the works of [19] and [20]. Besides, most properties of solutions exhibited by the introduction of time delay to nonlinear infectious disease model splits and causes destabilization of equilibrium point, such as birth and death rates of periodic and oscillatory solutions. The bifurcation analysis and stability switches of nonlinear solutions have recently attracted the attention of different authors while investigating the qualitative properties of delay systems (see [20] and [21]). However, the case where linearization method does not apply in the investigation of qualitative behavior of infectious disease with delay has not been sufficiently considered by several authors as noted in [1] and [22]. In this regard, it becomes necessary to further investigate the stability analysis of delay model where linearization method of analysis fails. Also, results of previous stability analysis showed that conditions for Hopf bifurcation of dynamical systems are sufficient but not necessary as models where linearization method fail are unable to stabilize the unstable interior non-hyperbolic equilibrium point. In addition, previous authors on SIR infectious disease model submitted that some ecological models such as predator-prey share same framework of modeling with epidemiological systems as seen in the works of [2], [6] and [22].

This paper therefore provides analytical findings and control measure of parameter values of

infectious disease reduced delay model that are slow and difficult to handle.

This paper is organized as follows: the second section which precedes section one modified an existing SIR disease model with discrete time delay being defined on it. Section 3 investigated the stability properties and determine conditions for qualitative behavior of solutions of the models. The fourth section investigated stability analysis of the transformed operator differential equation of the interior non-hyperbolic disease reduced delay model while employing the centre manifold theory. Numerical simulations are given in section 5 to validate analytical results from the models. The summary is given in section 5.2. This is followed by the interpretation and conclusion in 5.3.

2 Problem Formulation

2.1 The Mathematical Epidemic Model

This study considers the popular susceptible, infectious and recovered (SIR) epidemic model of the form [23].

$$\left. \begin{aligned} \frac{dS}{dt} &= \pi - \beta SI - \mu S \\ \frac{dI}{dt} &= \beta SI - (\gamma + \mu)I \\ \frac{dR}{dt} &= \gamma I - \mu R \end{aligned} \right\} \quad (1)$$

where,

$S(t_0) = S_0 > 0$, $I(t_0) = I_0 > 0$ and $R(t_0) = R_0 > 0$. The dependent variables S, I and R are the total susceptible category of people, total infected group and the total category of people who recovered from the disease. The parameter π represents the recruitment rate into the population, β is the transmission rate and μ is the sum of natural death rate and death rate due to the disease, while γ is the recovery rate. The nonnegative reproduction number R_0 is defined in (1). The work of previous authors guaranteed the existence of feasibility conditions for DFE and endemic stability analysis of (1). The DFE point is unstable if $R_0 > 1$ while the nontrivial equilibrium point exists if $R_0 > 1$ without delay. In the work of [24], the case where linearization method failed with and without delay in (1) was not studied. This can likely affect realistic results of the behavior of (1). The investigation of (1) with delay for further stability analysis falls within the scope of this study. Motivated by (1) and its associated previous assumptions, the study considered the delay form of model (1) which takes the form:

$$\left. \begin{aligned} \frac{dS}{dt} &= \pi - \beta SI - \mu S \\ \frac{dI}{dt} &= \beta S(t - \tau)I - (\gamma + \mu)I \\ \frac{dR}{dt} &= \gamma I - \mu R, \end{aligned} \right\} \quad (2)$$

where the admissible initial conditions are given by: $S(t_0) = S_0(t_0) > 0$, $I(t_0) = I_0(t_0) > 0$ and $R(t_0) = R_0(t_0) > 0$ with $t_0 \in [0, \tau]$, $\tau > 0$.

The domain of (2) is $\mathbb{R}_{+0}^3 = [S, I, R: S \geq 0, I \geq 0, R \geq 0]$ as in previous works. The introduction of intracellular delay parameter to (1) and the derivation of separable new generation matrix (NGM) make the study of equation (2) more realistic and ensure non instantaneous occurrences in the emergence of epidemic diseases. Again, the study of (2) by previous authors failed to investigate the model when the popular Hartman-Grobman's theorem is not satisfied. The flow chart of (2) is represented in the schematic diagram as shown in Figure 1.

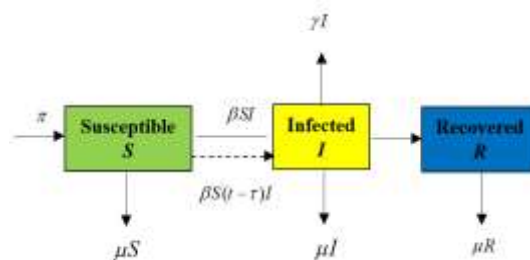


Fig. 1: Block diagram of system (2), [21]

As in the works of previous scholars (see [25], [26], [27], [28] and [29]) among others, the feasibility properties and stability analysis of (2) are verified where conditions for more general Hopf bifurcation analysis are derived. This study further re-formulates (2) and investigated the reduced functional operator differential equation (RFOpDEs) for a more general qualitative behavior when the closed curve splits using bifurcation maps for the centre manifold theorem (CMT) of analysis. The reduced OpDE further provides conditions under which a family of periodic solutions bifurcates from positive equilibrium for a more general analysis of qualitative behavior of (2).

2.2 The Reduced Form of System (2)

Since the population size of (2) is assumed constant, the qualitative equilibrium points satisfy $N = S + I + R$ such that $\frac{dN}{dt} = \frac{dS}{dt} + \frac{dI}{dt} + \frac{dR}{dt} = 0$. For dimensional reduction, we can drop the variable R since $R = N - S - I$ such that the dynamics of the

reduced form of (2) is determined by the first two equations of the form:

$$\begin{aligned} \frac{dS}{dt} &= \pi - \beta S(t)I(t) - \mu S(t) \\ \frac{dI}{dt} &= \beta S(t - \tau)I(t) - (\gamma + \mu)I(t) \end{aligned} \quad (3)$$

The variables and parameters of (3) are the same as those considered in (1) and (2). The admissible initial conditions of (3) are given by $S(t_0) = \phi_1(t_0)$, $I(t_0) = \phi_2(t_0)$ for $\phi_i(t_0) \geq 0$, where $t_0 \in [-\tau, 0]$, $\phi_i(0) > 0$ ($i = 1, 2$), $\tau > 0$ and $(\phi_1(t_0), \phi_2(t_0)) \in C([-\tau, 0], \mathbb{R}_+^2)$, where C is the Banach space of continuous mapping from $[-\tau, 0]$ into \mathbb{R}_+^2 . The assumptions on the reduced form of (3) are alike to (1) and (2) above. The flow chart for (3) is represented by Figure 2.

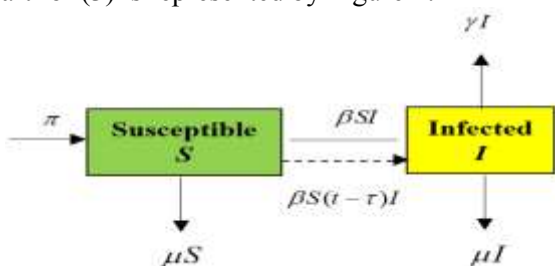


Fig. 2: Block diagram of (3), see [21]

For (3) to be meaningful, the feasibility conditions are verified and conditions of Hopf bifurcations are derived as.

Theorem 1: The dependent variables $S(t)$ and $I(t)$ at time t of (3) are non-negative.

Proof: Since scalar ordinary differential equations (ODEs) can be written as first order equations such that the new dependent variable can be written in vector form, system (3) can be expressed as

$$T = \text{col}(S, I) \in \mathbb{R}_+^2,$$

where

$$(\phi_1(t_0), \phi_2(t_0)) \in C([-\tau, 0], \mathbb{R}_+^2), x_i(t_0) = \phi_i(t_0) \geq 0, \phi_i(0) > 0 \quad (i = 1, 2).$$

We can define

$$F(T) = \begin{pmatrix} F_1(T) \\ F_2(T) \end{pmatrix} = \begin{pmatrix} \pi - \beta SI - \mu S \\ \beta S(t - \tau)I - (\gamma + \mu)I \end{pmatrix}$$

from which (3) becomes a differential equation of the form

$$\frac{dT}{dt} = F(T), \quad (4)$$

with initial conditions that $T(t_0) = (\phi_1(t_0), \phi_2(t_0)) \in C([-\tau, 0], \mathbb{R}_+^2)$, $\phi_i(0) > 0$ ($i = 1, 2$). Equation (4) can be verified such that whenever the complex solution is expressed in terms of real vectors $T(t_0) \in \mathbb{R}_+^2$ such that if the variables S and I are both homogeneous, then

$$F_i(T)|_{x_i=0, T \in \mathbb{R}_+^2} > 0,$$

where $\mathbb{R}_+^2 = \{(x_1, x_2 | x_i \geq 0), i = 1, 2\}$ with $x_1 = S(t)$, $x_2 = I(t)$. From lemma [28], any solution of (4) with $T(t_0) \in \mathbb{C}_+$, $T(t, T(t_0)) \in \mathbb{R}_+^2 \quad \forall t \geq 0$. Thus, the solution of (3) exists in \mathbb{R}_+^2 and remains positive $\forall t > 0$.

The following theorems ensure the positivity and boundedness property of (3).

Theorem 2: For admissible positive initial conditions, the solutions of (3) are positive $\forall t \geq 0$.

Proof: From first equation of (3), i.e.,

$$\frac{dS}{dt} = \pi - \beta SI - \mu S.$$

Let $S(t) > 0 \quad \forall t > 0$. Suppose this is not the case, then there exists $t_1 > 0$ and $\varepsilon_1 > 0$ for which $S(t) > 0$ at $t < t_1$, $S(t) = 0$ at $t = t_1$ and $S(t) < 0$ for $t \in [t_1, t_1 + \varepsilon_1)$. Therefore,

$$\begin{aligned} \left. \frac{dS}{dt} \right|_{t=t_1} &= \pi - \beta S(t_1)I(t_1) - \mu S(t_1). \\ \left. \frac{dS}{dt} \right|_{t=t_1} &= \pi > 0. \end{aligned}$$

This is a contradiction. So $S(t)$ is positive $\forall t > 0$. Given the second equation of (3),

$$\frac{dI(t)}{I(t)} = [\beta S(t - \tau) - (\gamma + \mu)],$$

on integrating both sides with the given initial values using Gronwall-Bellman's inequality [29] we have:

$$I(t) = I(t_0)e^{\int_{t_0}^t [\beta S(v - \tau) - (\gamma + \mu)] dv}.$$

Thus,

$I(t) > 0 \quad \forall t > 0$, since $I(t_0) > 0$ and exponential is always positive. Thus, theorem (2) holds.

Theorem 3: The solutions of (3) are ultimately bounded.

Proof:

Since solutions of (3) exist in \mathbb{R}_+^2 and remains positive $\forall t > 0$, then $N'(t) = S'(t) + I'(t)$ yields $N'(t) = \pi - \mu S(t) - (\gamma + \mu)I(t) - \beta I(t)(S(t) - S(t - \tau))$, the solutions at $S(t)$ and $S(t - \tau)$ cannot approach zero but some positive limit which can be determined by the initial history as in [25]. Thus,

$$N'(t) \leq \pi - (\mu S(t) + (\gamma + \mu)I(t)).$$

Define $\xi > 0 = \min \{\mu, \gamma + \mu\}$.

The linear differential inequality takes the form

$$N'(t) + \xi N(t) \leq \pi.$$

The analytical solution of the resulting linear differential inequality yields a solution of the form

$$N(t) \leq \frac{\pi}{\xi} + \left(N(0) - \frac{\pi}{\xi} \right) e^{-\xi t}, \text{ and}$$

$$\lim_{t \rightarrow \infty} N(t) \leq \frac{\pi}{\xi},$$

and the theorem is satisfied. Thus, the system (3) is well formulated both epidemiologically and

mathematically. For purpose of further stability analysis of (3), we state the following working definitions.

Definition 1

The non-negative reproduction number, R_0 of (3) is the product of the infection rate and the mean duration of the infection of the DFE at E_0 . If the DFE at E_0 of (3) exists and stable, the linearized form of (3) splits to the form

$$\frac{dx_i}{dt} = \mathcal{F}_i(x) - \mathcal{V}_i(x), i = 1, 2,$$

where $\mathcal{F}_i(x)$ is the rate of appearance of new infectious in component i ($i = 1, 2$) and $\mathcal{V}_i(x)$ is the rate of other interactions between component i and other infected components. For epidemic calculation of reproduction number R_0 , see the publications of [14] and [30].

Definition 2

For more general Hopf Bifurcation when linearization matrix has at least one eigenvalue with zero real part, the study provides the desired invariant subspace required for further stability analysis. The invariant simple closed curve splits and attracts periodic orbits when the origin is unstable and repelling when the origin is stable, otherwise periodic solutions exist. This study applies the dynamical system with the possibility of having attracted periodic orbits on the invariant circle for the bifurcation maps, [31].

3 Stability Analysis of Disease model

3.1 Stability Analysis For (3)

For stability analysis of (3), we can determine the DFE point and the endemic equilibrium point.

3.2 The Disease-Free Equilibrium (DFE) Point

Lemma 1: The DFE point of (3) occurs without delay at $E_0(S_0, I_0) = E_0\left(\frac{\pi}{\mu}, 0\right)$.

Proof: The DFE at $E_0\left(\frac{\pi}{\mu}, 0\right)$ of (3) satisfies the conditions

$$\begin{aligned} \pi - \beta SI - \mu S &= 0 \\ \beta SI - (\gamma + \mu)I &= 0 \end{aligned} \tag{5}$$

where $S_0 = \frac{\pi}{\mu}$ and $I_0 = 0$. Thus, the DFE of (3) occurs at $E_0\left(\frac{\pi}{\mu}, 0\right)$.

Theorem 4: The DFE at $E_0\left(\frac{\pi}{\mu}, 0\right)$ of (3) without delay is locally asymptotically stable.

Proof: The non-zero reliable Jacobian matrix of (3) at $E_0\left(\frac{\pi}{\mu}, 0\right)$ yields

$$J(E_0) = \begin{pmatrix} -\mu & 0 \\ 0 & -(\gamma + \mu) \end{pmatrix} \tag{6}$$

From linear algebra theory, the non-zero displacement amplitude of $J(E_0)$ is given by

$$|J(E_0) - \lambda I_2| = 0 \tag{7}$$

where I_2 is the associated 2×2 unit matrix of (3). The associated characteristic polynomial of (7) yields two eigenvalues: $\lambda_1 = -\mu$ and $\lambda_2 = -(\gamma + \mu)$. Clearly, λ_1 and λ_2 are negative and by Routh-Hurwitz criterion the DFE is locally asymptotically stable, [32].

For non-trivial stability analysis of (3), we assume that the disease has entered the population and calculate the popular reproductive number R_0 of the infectious epidemic model. This dimensionless reproductive number R_0 provides the threshold quantity for control of the infectious disease and is defined epidemiologically as the number of infectives who got infected because of existing single infective [30] and [33]. We calculate the epidemiological R_0 of (3) as $R_0 = \frac{\pi\beta}{\mu(\gamma + \mu)}$ using definition 1 above.

Theorem 5: The system (3) with $\tau = 0$ is a stable node when $R_0 < 1$ and a saddle when $R_0 > 1$ at $E_0\left(\frac{\pi}{\mu}, 0\right)$.

Proof: The non-zero Jacobian matrix of (3) when $\tau = 0$ at $E_0\left(\frac{\pi}{\mu}, 0\right)$ for the $R_0 = \frac{\pi\beta}{\mu(\gamma + \mu)}$ yields

$$J_{E_0} = \begin{pmatrix} -\mu & \frac{\pi\beta}{\mu} \\ 0 & (\gamma + \mu)(R_0 - 1) \end{pmatrix} \tag{8}$$

The associated characteristic equation of (8) becomes

$$|\lambda I_2 - J_{E_0}| = 0 \tag{9}$$

where I_2 is the identity matrix of (3) and λ the characteristic root. From (9), the characteristic equation is given by $(\lambda + \mu)(\lambda - (\gamma + \mu)(R_0 - 1)) = 0$ with two eigenvalues given by $\lambda_1 = -\mu$ and $\lambda_2 = (\gamma + \mu)(R_0 - 1)$. Clearly, λ_1 is always negative while $\lambda_2 < 0$ when $R_0 < 1$ (stable node) and $\lambda_2 > 0$ when $R_0 > 1$ (saddle). Hence Theorem 5 holds.

Note that if $\lambda_2 \neq 0$, the solutions of (3) and consequently (5) exist and satisfy the Hartman-Grobman's theorem [26]. However, linearization method fails when $R_0 = 1$ in which case $\lambda_2 = 0$. This makes the normal form concept (NFC) and the

center manifold theorem (CMT) possible where at least one of the eigenvalues is zero, see [22].

3.3 Stability Analysis of DFE When $R_0 = 1$ For (3)

From (9), one of the eigenvalues of (3) is zero and the other is negative when evaluated at $R_0 = 1$. For $R_0 = 1$ and $\lambda_2 = 0$ (9) satisfies the conditions of [33]. In other words, at $R_0 = 1$, the DFE of a more general Hopf bifurcation of definition 2 determines the direction and period of system (3) using the Center Manifold Theorem (CMT) analysis.

Theorem 6: The system given by (3) undergoes forward bifurcation at $E_0\left(\frac{\pi}{\mu}, 0\right)$ when R_0 crosses one.

Proof: When $R_0 = 1$, then $\frac{\pi\beta}{\mu(\gamma+\mu)} = 1$ and the DFE at $E_0\left(\frac{\pi}{\mu}, 0\right)$ corresponds to $\beta = \frac{\mu(\gamma+\mu)}{\pi} = \beta^*$. From the qualitative behavior of (3), we observe that one of the eigenvalues is zero and the other is negative at $R_0 = 1$ when $\beta = \beta^*$. Since linearization method cannot hold, the center manifold theorem (CMT) for more general invariant circle is employed for its stability analysis as in [32].

For the transformation of (3), the study introduced the variables $s = S$ and $i = I$, where

$$\begin{aligned} \frac{ds}{dt} &= \pi - \beta si - \mu s && \doteq f_1 \\ \frac{di}{dt} &= \beta s(t - \tau)i - (\gamma + \mu)i && \doteq f_2 \end{aligned} \quad (10)$$

Let $\beta = \beta^*$ be the bifurcation parameter and (J_A^*) the Jacobian matrix at $R_0 = 1$ such that

$$(J_A^*) = \begin{pmatrix} -\mu & -\frac{\pi\beta^*}{\mu} \\ 0 & 0 \end{pmatrix}. \quad (11)$$

Let $v = [v_1, v_2]^T$ be the right required eigenvectors and $[u_1, u_2]$ be the left eigenvector of the Jacobian matrix corresponding to zero eigenvalue. The right eigenvectors at $\lambda = 0$ gives

$$v = (v_1, v_2) = \left(-\frac{\pi\beta^*}{\mu^2}, 1\right),$$

and the left-hand eigenvectors for $\lambda = 0$ becomes

$$u = (u_1, u_2) = (0, 1).$$

From right-hand and left-hand eigenvectors, the condition

$$u \cdot v = (0, 1) \cdot \left(-\frac{\pi\beta^*}{\mu^2}, 1\right) = 1$$

holds. The Hessian matrix of (3) takes the form

$$D^2_{sif} = \begin{pmatrix} \frac{\partial^2 f}{\partial s^2} & \frac{\partial^2 f}{\partial s \partial i} \\ \frac{\partial^2 f}{\partial i \partial s} & \frac{\partial^2 f}{\partial i^2} \end{pmatrix}.$$

at (E_0, β^*) from which the algebraic calculations of $D^2_{sif_2}$ take the form

$$\frac{\partial^2 f_2}{\partial s^2} \Big|_{(E_0, \beta^*)} = 0 \text{ and } \frac{\partial^2 f_2}{\partial i \partial s} \Big|_{(E_0, \beta^*)} = -\beta^*$$

and

$$\begin{aligned} \frac{\partial^2 f_2}{\partial i^2} \Big|_{(E_0, \beta^*)} &= 0 \text{ and } \frac{\partial^2 f_2}{\partial s \partial i} \Big|_{(E_0, \beta^*)} = \beta^*; \\ \frac{\partial^2 f_2}{\partial s \partial \beta} \Big|_{(E_0, \beta^*)} &= 0 \text{ and } \frac{\partial^2 f_2}{\partial i \partial \beta} \Big|_{(E_0, \beta^*)} = -\frac{\pi}{\mu} \end{aligned}$$

while

$$\frac{\partial^2 f_2}{\partial s \partial \beta} \Big|_{(E_0, \beta^*)} = 0 \text{ and } \frac{\partial^2 f_2}{\partial i \partial \beta} \Big|_{(E_0, \beta^*)} = \frac{\pi}{\mu}.$$

Substituting the algebraic calculations for parameters p and q of [33], where f_k equals k^{th} component of f such that the coefficients are given by:

$$\begin{aligned} p &= \sum_{k,i,j=1}^n u_k v_i v_j \frac{\partial^2 f_k}{\partial s_i \partial i_j} \Big|_{(E_0, \beta^*)} = v_1^2 \frac{\partial^2 f_2}{\partial s^2} \Big|_{(E_0, \beta^*)} \\ &\quad + 2v_1 v_2 \frac{\partial^2 f_2}{\partial s \partial i} \Big|_{(E_0, \beta^*)} + v_2^2 \frac{\partial^2 f_2}{\partial i^2} \Big|_{(E_0, \beta^*)} \\ &= \left(\frac{-\beta^* \pi}{\mu}\right)^2 (0) + 2\left(\frac{-\beta^* \pi}{\mu^2}\right) (1)(\beta^*) + (1)^2 (0) \\ &= -\frac{2\beta^{*2} \pi}{\mu^2} < 0, \text{ and} \end{aligned}$$

$$\begin{aligned} q &= \sum_{k,i=1}^n u_k v_i \frac{\partial^2 f_k}{\partial x_i \partial \phi_j} \Big|_{(E_0, \beta^*)} \\ &= v_1 \frac{\partial^2 f_2}{\partial s \partial \beta} \Big|_{(E_0, \beta^*)} + v_2 \frac{\partial^2 f_2}{\partial i \partial \beta} \Big|_{(E_0, \beta^*)} \\ &= \left(\frac{-\beta^* \pi}{\mu^2}\right) (0) + (1) \left(\frac{\pi}{\mu}\right) = \frac{\pi}{\mu} > 0. \end{aligned}$$

Since p is negative and q is positive, the forward (supercritical) bifurcation occurs when R_0 crosses unity from below with small positive asymptotically stable equilibrium where the DFE losses its stability as observed in [33] and [34].

3.4 Stability of Endemic Equilibrium of (3)

For stability of endemic disease, we restrict our attention on the existence of endemic equilibrium at $E^*(S^*, I^*)$ of (3). When $R_0 > 1$, the endemic equilibrium points at $E^*(S^*, I^*)$ occurs when the disease persists in the population.

Lemma 2: The stability of endemic equilibrium at $E^*(S^*, I^*) = E^*\left(\frac{\gamma+\mu}{\beta}, \frac{\pi\beta-\mu(\gamma+\mu)}{\beta(\gamma+\mu)}\right)$ of (3) occurs when the disease persists in the population without delay.

Proof: The endemic equilibrium of (3) at $E^*(S^*, I^*)$ satisfies $\frac{ds}{dt} = \frac{di}{dt} = 0$. This condition yields

$$\begin{aligned} \pi - \beta SI - \mu S &= 0, \\ [\beta S - (\gamma + \mu)]I &= 0. \end{aligned} \quad (12)$$

When $I \neq 0$, the second equation of (12) yields $S^* = \frac{\gamma + \mu}{\beta}$ and the corresponding first equation of (12) yields $I^* = \frac{\pi\beta - \mu(\gamma + \mu)}{\beta(\gamma + \mu)}$. Thus, the endemic equilibrium points of (12) occur at E^* for $I \neq 0$.

Theorem 7: The endemic equilibrium at $E^*(S^*, I^*)$ of (3) is locally asymptotically stable without delay if the disease infection rate is greater than the deaths sum *i.e.*, $\beta\pi - \mu(\gamma + \mu) > 0$.

Proof: The endemic equilibrium $E^*(S^*, I^*)$ of (3) occurs at $E^*\left(\frac{\gamma + \mu}{\beta}, \frac{\pi\beta - \mu(\gamma + \mu)}{\beta(\gamma + \mu)}\right)$. The linearized Jacobian matrix of (3) at $E^*\left(\frac{\gamma + \mu}{\beta}, \frac{\pi\beta - \mu(\gamma + \mu)}{\beta(\gamma + \mu)}\right)$ yields

$$J^*(E^*) = \begin{pmatrix} -\left(\frac{\pi\beta}{\gamma + \mu}\right) & -(\gamma + \mu) \\ \left(\frac{\pi\beta - \mu(\gamma + \mu)}{\gamma + \mu}\right) & 0 \end{pmatrix} \quad (13)$$

The non-zero amplitude of $J^*(E^*)$ becomes

$$|J^*(E^*) - \lambda I| = 0, \quad (14)$$

from which the characteristic polynomial of (14) yields

$$\lambda^2 + \frac{\pi\beta}{\gamma + \mu}\lambda + (\pi\beta - \mu(\gamma + \mu)) = 0 \quad (15)$$

where $a_1 = \frac{\pi\beta}{\gamma + \mu}$ and $a_2 = \pi\beta - \mu(\gamma + \mu)$.

The roots of (15) yields

$$\lambda_{1,2} = \frac{-a_1 \pm \sqrt{a_1^2 - 4a_2}}{2}.$$

For persistency of epidemics, $\pi\beta - \mu(\gamma + \mu) > 0$, *i.e.*, $\frac{\pi\beta}{\mu(\gamma + \mu)} > 1$. Thus,

$a_1^2 - 4a_2$ is either smaller or greater than $\left(\frac{\pi\beta}{\gamma + \mu}\right)^2$.

Suppose $\left(\frac{\pi\beta}{\gamma + \mu}\right)^2 < 4(\pi\beta - \mu(\gamma + \mu))$, the complex eigenvalues have negative real parts. Also, if $\left(\frac{\pi\beta}{\gamma + \mu}\right)^2 > 4(\pi\beta - \mu(\gamma + \mu))$, $a_1^2 - 4a_2$ must be smaller in absolute value than $\left(\frac{\pi\beta}{\gamma + \mu}\right)^2$ and still the real part is negative. In either way, we conclude that the endemic equilibrium is stable if $R_0 > 1$ since the real parts of both eigenvalues are negative.

3.5 The Hopf Bifurcation Analysis of Endemic Equilibrium Point of (3)

For further stability analysis, the study investigated the behavior of (3) using the characteristic equation (15) using the theorem below.

Theorem 8: Suppose (3) is locally asymptotically stable at $E^*(S^*, I^*)$ with $\pi\beta - \mu(\gamma + \mu) > 0$, then the following result holds. If $\pi\beta < \gamma + \mu$, then there

exists $\tau_c = \tilde{\tau} > 0$, a critical delay points such that if $\tau \in [0, \tilde{\tau})$ all the roots of (3) have negative real part. When $\tilde{\tau} = \tau_c$, system (3) bifurcates with purely imaginary roots $\pm i\omega_+$ and at $\tau > \tilde{\tau}$ where equation (15) has at least one root with positive real part.

Proof: For stability analysis of the endemic equilibrium point at $E^*(S^*, I^*)$ of system (3) with delay, we define the following generic terms for the purpose of transformation.

$$S^*(t) = S(t) - E^* \text{ and } I^*(t) = I(t) - E^*.$$

where E^* is the positive (endemic) equilibrium point. The system (3) can be transformed to the linearised system as

$E^*(S^*, I^*) = E^*\left(\frac{\gamma + \mu}{\beta}, \frac{\pi\beta - \mu(\gamma + \mu)}{\beta(\gamma + \mu)}\right)$ to form in which the decomposed Jacobian matrix at the positive equilibrium point given by

$$J^*_A + J^*_B e^{-\lambda\tau} = \begin{pmatrix} S^*(t) \\ I^*(t) \end{pmatrix} + \begin{pmatrix} S^*(t - \tau) \\ I^*(t - \tau) \end{pmatrix},$$

where

$$J^*_A = \begin{pmatrix} -\frac{\pi\beta}{\gamma + \mu} & -(\gamma + \mu) \\ 0 & 0 \end{pmatrix}$$

and

$$J^*_B e^{-\lambda\tau} = \begin{pmatrix} 0 & 0 \\ \left(\frac{\pi\beta - \mu(\gamma + \mu)}{\gamma + \mu}\right) e^{-\lambda\tau} & 0 \end{pmatrix}.$$

Hence,

$$J^*_A + J^*_B e^{-\lambda\tau} = \begin{pmatrix} -\frac{\pi\beta}{\gamma + \mu} & -(\gamma + \mu) \\ \left(\frac{\pi\beta - \mu(\gamma + \mu)}{\mu}\right) e^{-\lambda\tau} & 0 \end{pmatrix}.$$

For stability analysis of (3) at $E^*(S^*, I^*)$, the associated reliable Jacobian matrix takes the form

$$|\lambda I - J_A - e^{-\lambda\tau} J_B| = 0.$$

Hence

$$\lambda^2 + \left(\frac{\pi\beta}{\gamma + \mu}\right)\lambda + (\pi\beta - \mu(\gamma + \mu))e^{-\lambda\tau} = 0$$

can be put in the form

$$\lambda(\tau) = \lambda^2 + a_1\lambda + a_2 + a_3 e^{-\lambda\tau} = 0 \quad (16)$$

where

$$a_1 = \frac{\pi\beta}{\gamma + \mu}, \quad a_2 = 0 \quad \text{and} \quad a_3 = \pi\beta - \mu(\gamma + \mu).$$

Clearly, at $\tau = 0$, (16) becomes (15) and

$$\lambda^2 + a_1\lambda + (a_2 + a_3) = 0.$$

Since $\pi\beta > \mu(\gamma + \mu)$ at $\tau = 0$ both roots of (16) will be negative and so by Routh-Hurwitz criterion system (3) is locally asymptotically stable.

Next, the study derives the conditions for Hopf bifurcation by showing that a pair of purely imaginary roots $\lambda = \pm i\tilde{\omega}$ exists. Let $\lambda = i\tilde{\omega}$ be such that (16) yields:

$$-\tilde{\omega}^2 + a_1 i \tilde{\omega} + a_2 + a_3(\cos \tilde{\omega} \tau - i \sin \tilde{\omega} \tau) = 0 \quad (17)$$

where $a_2 = 0$.

Solving equation (17) for the real part, we have

$$-\tilde{\omega}^2 + a_2 = -a_3 \cos \tilde{\omega} \tau \quad (18)$$

and similarly, from (17), the imaginary part yields

$$a_1 \tilde{\omega} = a_3 \sin \tilde{\omega} \tau. \quad (19)$$

Summing the squares of real and imaginary parts of (18) and (19) yield

$$\tilde{\omega}^4 + (a_1 - 2a_2)\tilde{\omega}^2 + (a_2^2 - a_3^2) = 0. \quad (20)$$

The roots of (20) are given by:

$$\tilde{\omega}_+^2 = -\frac{1}{2}(a_1 - 2a_2) \pm \frac{1}{2}\sqrt{(a_1 - 2a_2)^2 - 4(a_2^2 - a_3^2)}.$$

If $a_1 < 0$, then (20) has positive real roots when τ takes some critical value. Thus, Hopf bifurcation occurs as τ passes through the critical value $\tilde{\tau}$. If conditions of Theorem (8) are satisfied, then there exists a critical delay $\tilde{\tau}$ such that the infected steady state at E^* of (3) is asymptotically stable when $\tau \in [0, \tilde{\tau})$ and unstable when $\tau > \tilde{\tau}$. From (18), we have purely imaginary roots $\lambda = \pm i\omega_k$ whenever $\tilde{\tau}_k (k = 0, 1, 2, \dots)$ such that

$$\tilde{\omega}_k + a_2 = -a_3 \cos \tilde{\omega} \tau_k$$

and the sequence of critical delay points yields

$$\tau_k = \frac{1}{\tilde{\omega}_k} \arccos \left[\frac{\tilde{\omega}_k^2 - a_2}{a_3} \right] + \frac{2\pi k}{\tilde{\omega}_k}, k = 0, 1, 2, \dots \quad (21)$$

At $k = 0$, the threshold delay margin yields the form

$$\tilde{\tau} = \frac{1}{\tilde{\omega}_0} \arccos \left[\frac{\tilde{\omega}_0^2 - a_2}{a_3} \right].$$

Thus at $\tau = \tau_k = \tilde{\tau}$, equation (16) has a pair of purely imaginary roots $\pm i\tilde{\omega}$ which are simple while all other roots have negative real parts. Therefore, at $\tau = \tau_k = \tilde{\tau}$, Hopf bifurcation occurs as τ passes through the critical value $\tilde{\tau}$.

We next verify the transversality condition using the following lemma

Lemma 3: Suppose conditions of Theorem (8) and $a_3 \cos \tilde{\omega}_0 \tau_k > 0$ are satisfied, then equation (15) has purely imaginary roots given by $\lambda = \pm i\omega_k$ whenever $\tilde{\tau}_k (k = 0, 1, 2, \dots)$. Then (2) is stable if $\tilde{\tau} \in [0, \tilde{\tau}_k)$, unstable for $\tau \geq \tau_k$ and undergoes Hopf bifurcation analysis at $\tau_k = \tilde{\tau}$, such that the transversality condition

$$Re \left[\frac{d\lambda}{d\tau} \right]_{\lambda = \pm i\omega_k, \tau = \tau_k} = \frac{a_3}{2e^{i\omega_k \tau_k}} > 0 \text{ holds.}$$

Proof: From the transcendental equation of (15), we apply the transversality condition to verify Hopf bifurcation for the sensitivity analysis.

Suppose $\lambda(\tau) = \sigma(\tau) + i\omega(\tau)$ ($\omega \in \mathbb{R}_+$) for (16) near $\tau = \tilde{\tau}_k, k = 0, 1, 2, \dots$ such that $\sigma(\tilde{\tau}_k) = 0$ and $\omega(\tilde{\tau}_k) = \tilde{\omega}_k$. Let

$$\lambda(\tau) = \lambda^2 + a_1 \lambda + a_2 + a_3 e^{-\lambda \tau}.$$

Differentiating the above implicitly, we have

$$\frac{d\lambda}{d\tau} = 2\lambda \frac{d\lambda}{d\tau} + a_1 \frac{d\lambda}{d\tau} + a_3 \left[e^{-\lambda \tau} \left(-\tau \frac{d\lambda}{d\tau} - \lambda \right) \right], i.e.,$$

$$\frac{d\lambda}{d\tau} = \frac{a_3 \lambda e^{-\lambda \tau}}{2\lambda + a_1 - a_3 \lambda e^{-\lambda \tau} - 1}$$

$$\left[\frac{d\lambda}{d\tau} \right]^{-1} = \frac{2\lambda + a_1 - a_3 \lambda e^{-\lambda \tau} - 1}{a_3 \lambda e^{-\lambda \tau}}$$

$$\left[\frac{d\lambda}{d\tau} \right]^{-1} = \frac{2}{a_3 e^{-\lambda \tau}} + \frac{a_1}{a_3 \lambda e^{-\lambda \tau}} - \frac{a_3 \tau e^{-\lambda \tau}}{a_3 \lambda e^{-\lambda \tau}} - \frac{1}{a_3 \lambda e^{-\lambda \tau}}$$

On replacing $\lambda = i\omega_k$, and $\tau = \tau_k, k = 0, 1, 2, \dots$, we have

$$Re \left[\frac{d\lambda}{d\tau} \right]_{\lambda = i\omega_k, \tau = \tau_k}^{-1} = \frac{2}{a_3 e^{-i\omega_k \tau_k}}$$

and on inverting back we have

$$\left[\frac{d\lambda}{d\tau} \right]_{\lambda = i\omega_k, \tau = \tau_k} = \frac{a_3}{2e^{i\omega_k \tau_k}} > 0$$

So $\lambda = \pm i\omega_k$ move towards \mathbb{C}_+ . Hence, the transversality condition holds at $\tau = \tau_k = \tilde{\tau}$.

The stability conditions for a more general Hopf bifurcation analysis of (3) are displayed in section 4.2 using numerical simulations on a specific example as can be seen in Figure 3, Figure 4, Figure 5, Figure 6, Figure 7, Figure 8, Figure 9, Figure 10, Figure 11, Figure 12, Figure 13, Figure 14 and Figure 15.

4 The Center Manifold Analysis

4.1 Application of Center Manifold Theorem (CMT) For Disease Model

This section derives formulas for investigating the stability properties of periodic solutions bifurcating from the positive equilibrium E^* at $\tau = \tilde{\tau}$ of (3) using the normal form concept and the center manifold theorem introduced in [33]. From previous section and the hypothesis of Definition 2, there is the need to characterize stability at a pair of purely imaginary roots of (15) and introduce coordinate transformation of (3).

Let $e_1 = s - S^*$, $e_2 = i - I^*$, where S^* and I^* are the nontrivial (endemic) equilibrium point. The system (3) can be transformed into the form:

$$\begin{aligned} \frac{de_1}{dt} &= \pi - \beta s i - \mu s \\ \frac{de_2}{dt} &= \beta s (t - \tau) i - (\gamma + \mu) i \end{aligned} \quad (22)$$

where $s = e_1 + S^*$, $i = e_2 + I^*$. Assume $\tau \in (0, \tilde{\tau})$ and let $t \rightarrow (t\tilde{\tau})$ be the time dependent delay. Assume that $\tilde{e}_i(t) = e_i(t\tilde{\tau}), i = 1, 2$. Let $\bar{\tau} = \tilde{\tau} + \sigma$, $\sigma \in \mathbb{R}$. Then $\sigma = 0$ is a Hopf bifurcation value for (22) and $e(t) = (s(t), i(t))^T$.

The system (22) gives the coordinate transformation of (3). Let $E^* = (s^*, i^*)$ denote the

endemic equilibrium point. From previous section, the endemic equilibrium points of (22) yield $E^* \left(\frac{\gamma+\mu}{\beta}, \frac{\pi\beta-\mu(\gamma+\mu)}{\beta(\gamma+\mu)} \right)$ such that the derived linear and nonlinear Jacobian matrices are given by the forms

$$J_{E^*} = \begin{pmatrix} -\frac{\pi\beta}{(\gamma+\mu)} & -(\gamma+\mu) \\ \left(\frac{\pi\beta-\mu(\gamma+\mu)}{(\gamma+\mu)}\right) e^{-i\tilde{\omega}\tilde{\tau}} & -(\gamma+\mu) \end{pmatrix},$$

and

$$N_1 = \begin{pmatrix} -\beta si \\ \beta s(t-\tau)i \end{pmatrix}.$$

The variational matrix of (22) can be decomposed into the following three sub matrices:

$$M_1 = \begin{pmatrix} -\frac{\pi\beta}{(\gamma+\mu)} & -(\gamma+\mu) \\ 0 & -(\gamma+\mu) \end{pmatrix},$$

$$M_2 = \begin{pmatrix} 0 & 0 \\ \left(\frac{\pi\beta-\mu(\gamma+\mu)}{(\gamma+\mu)}\right) & 0 \end{pmatrix} e^{-i\tilde{\omega}\tilde{\tau}}$$

and

$$N_1 = \begin{pmatrix} -\beta si \\ \beta s(t-\tau)i \end{pmatrix}, \quad (23)$$

where M_1 is the linear non-delayed matrix, M_2 is the linear delayed matrix and N_1 is the nonlinear matrix. From the perturbed variables of (22) and upon dropping the bars of the assumptions above, (22) can be re-written as functional differential equation (FDE) of the form $C([-1, 0], \mathbb{R}_+^2)$

$$\dot{e}(t) = M_\sigma(e_t) + N(\sigma, e_t), \quad (24)$$

where

$e_t = (e_1(t), e_2(t))^T \in \mathbb{R}_+^2$ is the solution of (22). $M_\sigma(e_t)$ and $N(\sigma)(e_t)$ are the linear and nonlinear transformations of (24) such that

$$M_\sigma: C([-1, 0], \mathbb{R}_+^2) \rightarrow \mathbb{R}_+^2,$$

and

$$N_1: R \times C([-1, 0], \mathbb{R}_+^2) \rightarrow \mathbb{R}_+^2 \text{ respectively,}$$

where,

$$M_\sigma(\Psi) = M_1\Psi(0) + M_2\Psi(-\tau) \text{ and}$$

$$N_1 = N(\sigma, \Psi) \text{ for } \Psi \in C([-1, 0], \mathbb{R}_+^2).$$

Equation (24) can be expressed as the sum of linear

$$M_\sigma(\Psi) \doteq (\tilde{\tau} + \sigma)M_1 \begin{pmatrix} \Psi_1(0) \\ \Psi_2(0) \end{pmatrix} + (\tilde{\tau} + \sigma)M_2 \begin{pmatrix} \Psi_1(-\tau) \\ \Psi_2(-\tau) \end{pmatrix} \quad (25)$$

and nonlinear functional given by

$$N_1 = N(\sigma, \Psi) \doteq (\tilde{\tau} + \sigma) \begin{pmatrix} -\beta\Psi_1(0)\Psi_2(0) \\ \beta\Psi_1(-\tau)\Psi_2(0) \end{pmatrix} \quad (26)$$

where

$$\Psi = (\Psi_1, \Psi_2)^T \in C([-1, 0], \mathbb{R}_+^2) \text{ and}$$

$$e_t(\rho) = e(t + \rho), \rho \in [-\tau, 0].$$

By Riesz Representation Theorem of [34], we define a bounded variation function

$$\eta(\rho, \sigma): [-\tau, 0] \rightarrow \mathbb{R}, \rho \in [-\tau, 0]$$

such that the linear operator can be expressed as

$$M_\sigma\Psi = \int_{-\tau}^0 d\eta(\rho, \sigma) \Psi(\rho) = \int_{-\tau}^0 [d\eta(\rho, \sigma)] (e(t + \rho)). \quad (27)$$

Equation (27) holds for $\Psi \in C([- \tau, 0], \mathbb{R}_+^2)$. Also, linear operators are equivalent to $n \times n$ squared matrices whose components are of bounded variation function of the form $\eta(\rho, \sigma): [-\tau, 0] \rightarrow \mathbb{R}_+^{n \times n}$, $\rho \in [-\tau, 0]$. The linear operator of (27) can be represented by bounded variation function of the form

$$\eta(\rho, \sigma): [-\tau, 0] \rightarrow \mathbb{R}_+^{2 \times 2}, \rho \in [-\tau, 0]$$

such that

$$\eta(\rho, \sigma) \doteq (\tilde{\tau} + \sigma)M_1\delta(\rho) + (\tilde{\tau} + \sigma)M_2\delta(\rho + \tau) \quad (28)$$

where (24) and (28) are expressed by

$$\eta(\rho, \sigma) = (\tilde{\tau} + \sigma) \begin{pmatrix} -\frac{\pi\beta}{(\gamma+\mu)} & -(\gamma+\mu) \\ 0 & -(\gamma+\mu) \end{pmatrix} \delta(\rho) + (\tilde{\tau} + \sigma) \begin{pmatrix} \frac{\pi\beta-\mu(\gamma+\mu)}{(\gamma+\mu)} & 0 \\ 0 & 0 \end{pmatrix} \delta(\rho + \tau).$$

Equation (25) is satisfied when $\sigma = 0$ and the Hopf bifurcation value for system (22) can be obtained. Since linear operators are equivalent to $n \times n$ squared matrices, for $\Psi \in C^1([- \tau, 0], \mathbb{R}_+^2)$, we can define the following matrix operators given by:

$$A(\sigma)\Psi(\rho) \doteq \begin{cases} \frac{d\Psi(\rho)}{d\rho}, & \rho \in [-\tau, 0) \\ \int_{-\tau}^0 d\eta(\rho, \sigma) \Psi(\rho), & \rho = 0 \end{cases},$$

where $A(\sigma) = Df$ is the Jacobian matrix evaluated at

a specified function and

$$N(\sigma)\Psi(\rho) \doteq \begin{cases} 0, & \rho \in [-\tau, 0) \\ N(\sigma, \Psi), & \rho = 0 \end{cases}.$$

From the analysis above, equation (22) is equivalent to the generalized matrix operator given by

$$\dot{e}_t = A(\sigma)e_t + N(\sigma)e_t \quad (29)$$

where

$$e_t(\rho) = e(t + \rho), \rho \in [-\tau, 0].$$

The operators A and N are the linear and nonlinear parts of (29). The equation (29) is called the normal form equation.

For the generalized matrix operator, we can write the solution e_t as the sum of vectors lying in the center subspace spanned by the eigenvectors corresponding to the eigenvalues $\lambda = \pm i\tilde{\omega}\tilde{\tau}$ projected to the center subspace. To accomplish this, we determine the adjoint of the operator A of ϕ denoted by $A^*\phi(s)$, where $*$ denotes is either the adjoint operator or transposed conjugate matrix. Thus, for $\phi \in C^1([0, \tau], (\mathbb{R}_+^2)^*)$ the adjoint operator A^* of ϕ can be defined as:

$$A^* \phi(s) = \begin{cases} \frac{-d\phi(s)}{ds}, & s \in (0, \tau] \\ \int_{-\tau}^0 d\eta^*(t, 0) \phi(-t), & s = 0 \end{cases}$$

For $\Psi \in C^1([-\tau, 0], \mathbb{R}_+^2)$ and $\phi \in C^1([0, \tau], \mathbb{R}_+^2)$, we can define a bilinear inner product to normalize the eigenvalues of A and A^* defined by

$$\langle \Phi(s), \Psi(\rho) \rangle = \bar{\Phi}(0)\Psi(0) - \int_{-\tau}^0 \int_{s=0}^{\rho} \bar{\Phi}(s - \rho) d\eta(\rho)\Psi(s) ds \quad (30)$$

where, $\Psi(\rho)$ lies in the original function space on $C([-\tau, 0], \mathbb{R}_+^2)$ and $\phi(s)$ lies on the adjoint function of the space defined on $C([-\tau, 0], \mathbb{R}_+^2)$ for $\eta(\rho) = \eta(\rho, 0)$ while $\bar{\Phi}$ is the complex conjugate of Φ . Since $\lambda = \pm i\tilde{\omega}\tilde{\tau}$ are eigenvalues of $A(0)$, they are also the eigenvalues of $A^*(0)$ as well. Thus, we can compute $\lambda = +i\tilde{\omega}\tilde{\tau}$ for $A(0)$ and $\lambda = -i\tilde{\omega}\tilde{\tau}$ for $A^*(0)$ respectively. Suppose that $b \in C^1$ is a one parameter eigenvector of $A(0)$ associated with eigenvalue $\lambda = i\tilde{\omega}\tilde{\tau}$ which $b(\rho) = (1, \zeta)^T e^{i\tilde{\omega}\tilde{\tau}\rho}$.

Thus, we have:

$$A(0)b(\rho) = i\tilde{\omega}\tilde{\tau}b(\rho) \quad \forall \rho \in C[-\tau, 0] \text{ at } \sigma = 0.$$

At $\rho = 0$, we can obtain $b(0) = (1, \zeta)^T$ such that

$$A(0)b(0) = i\tilde{\omega}\tilde{\tau}b(0) = i\tilde{\omega}\tilde{\tau}(1, \zeta)^T.$$

From the linear part of (29) at $\sigma = 0$, we have:

$$M_1 b(0) + M_2 b(-\tau) = i\tilde{\omega}\tilde{\tau}b(0).$$

This yields the equation of the form:

$$\tilde{\tau} \begin{pmatrix} -\frac{\pi\beta}{(\gamma+\mu)} & -(\gamma+\mu) \\ 0 & -(\gamma+\mu) \end{pmatrix} \begin{pmatrix} 1 \\ \zeta \end{pmatrix} + \tilde{\tau} \begin{pmatrix} 0 & 0 \\ \frac{\pi\beta-\mu(\gamma+\mu)}{(\gamma+\mu)} & 0 \end{pmatrix} \begin{pmatrix} 1 \\ \zeta \end{pmatrix} e^{-i\tilde{\omega}\tilde{\tau}} = i\tilde{\omega}\tilde{\tau} \begin{pmatrix} 1 \\ \zeta \end{pmatrix},$$

from which we have

$$\zeta = \frac{\left(\frac{\pi\beta-\mu(\gamma+\mu)}{(\gamma+\mu)}\right)e^{-i\tilde{\omega}\tilde{\tau}}}{i\tilde{\omega}+(\gamma+\mu)}.$$

Similarly, let $b^*(s) = \bar{D}(1, \zeta^*)e^{i\tilde{\omega}\tilde{\tau}s}$ be the eigenvector of A^* corresponding to $-i\tilde{\omega}\tilde{\tau}$ at $\sigma = 0$, where D can be determined. From the definitions of A^* , the linear form of (30) yields

$$M_1^* b^*(0) + M_2^* b^*(-\tau) = -i\tilde{\omega}\tilde{\tau}b^*(0).$$

The linear part of (29) yields

$$\tilde{\tau} \begin{pmatrix} -\frac{\pi\beta}{(\gamma+\mu)} & 0 \\ -(\gamma+\mu) & -(\gamma+\mu) \end{pmatrix} \begin{pmatrix} 1 \\ \zeta^* \end{pmatrix} + \tilde{\tau} \begin{pmatrix} 0 & \frac{\pi\beta-\mu(\gamma+\mu)}{(\gamma+\mu)} \\ 0 & 0 \end{pmatrix} \begin{pmatrix} 1 \\ \zeta^* \end{pmatrix} e^{i\tilde{\omega}\tilde{\tau}} = -i\tilde{\omega}\tilde{\tau} \begin{pmatrix} 1 \\ \zeta^* \end{pmatrix}$$

from which we have

$$\zeta^* = \frac{(\gamma+\mu)}{(i\tilde{\omega}-(\gamma+\mu))}.$$

To assure that $\langle b^*(s), b(\rho) \rangle = 1$, we can determine the value of D . By (30), the inner product is: expressed as

$$\langle B^*(s), b(\rho) \rangle = \bar{D} \bar{b}^*(0)b(0) - \int_{\rho=-\tau}^0 \int_{s=0}^{\rho} \bar{b}^*(s - \rho) d\eta(\rho)b(s) ds.$$

$$\begin{aligned} \text{Thus, } \langle B^*(s), b(\rho) \rangle &= \bar{D}(1, \bar{\zeta}^*)(1, \zeta)^T \\ &- \int_{-\tau}^0 \int_{s=0}^{\rho} \bar{D}(1, \bar{\zeta}^*)e^{-i\tilde{\omega}\tilde{\tau}(s-\rho)} d\eta(\rho)(1, \zeta)e^{i\tilde{\omega}\tilde{\tau}s} ds \\ &= \bar{D} \left\{ 1 + \zeta \bar{\zeta}^* + \right. \\ &\left. (1, \bar{\zeta}^*) \begin{pmatrix} 0 \\ \frac{\pi\beta-\mu(\gamma+\mu)}{(\gamma+\mu)} \end{pmatrix} \tilde{\tau} e^{-i\tilde{\omega}\tilde{\tau}} \right\} \\ &= \bar{D} \left\{ 1 + \zeta \bar{\zeta}^* + \tilde{\tau} \bar{\zeta}^* \left(\frac{\pi\beta-\mu(\gamma+\mu)}{(\gamma+\mu)} \right) e^{-i\tilde{\omega}\tilde{\tau}} \right\} \end{aligned}$$

$$\text{Thus, we can choose } \bar{D} = \frac{1}{1 + \zeta \bar{\zeta}^* + \tilde{\tau} \bar{\zeta}^* \left(\frac{\pi\beta-\mu(\gamma+\mu)}{(\gamma+\mu)} \right) e^{-i\tilde{\omega}\tilde{\tau}}}$$

such that

$$D = \frac{1}{1 + \bar{\zeta} \zeta^* + \tilde{\tau} \zeta^* \left(\frac{\pi\beta-\mu(\gamma+\mu)}{(\gamma+\mu)} \right) e^{i\tilde{\omega}\tilde{\tau}}}.$$

Next, we employ the notations of [18] and compute the coordinates to describe the center manifold C_0 of the operator retarded differential equation (OpRDE) when $\sigma = 0$.

Let e_t be the solution of (22) when $\sigma = 0$. From the definition of eigenvectors of operator A , we can introduce the state variables to calculate the coordinates to describe the actual center manifold C_0 of (3).

Define

$$z(t) = \langle b^*, e_t \rangle, W(t, \rho) = e_t(\rho) - 2R_e[z(t)b(\rho)], \quad (31)$$

where $W(t, \rho)$ is the rest of the solution which does not lie in the center subspace. From definition and the local expansion of stable manifold C_0 at $\sigma = 0$, we have

$$\dot{W} = W(z(t), \bar{z}(t), \rho), \rho = 0,$$

and by Taylor's series expansion, we have

$$\begin{aligned} \dot{W} &= W(0, 0) + W_z(0, 0)z + W_{\bar{z}}(0, 0)\bar{z} \\ &+ \frac{1}{2} [W_{zz}(0, 0)z^2 + 2W_{z\bar{z}}(0, 0)z\bar{z} + W_{\bar{z}\bar{z}}(0, 0)\bar{z}^2] \\ &+ \mathcal{O}(|z|^3 + |\bar{z}|^3) \end{aligned}$$

with the conditions that $W(0, 0) = W_z(0, 0) = W_{\bar{z}}(0, 0) = 0$ as in the hypothesis of the center manifold theorem (CMT). Also, from local stable manifold theory, we can express the center manifold C_0 by Taylor expansion of $\mathcal{O}(|z|^3)$ of the form

$$W(z(t), \bar{z}(t), \rho) = \left[W_{zz} \frac{z^2}{2} + W_{z\bar{z}} z\bar{z} + W_{\bar{z}\bar{z}} \frac{\bar{z}^2}{2} \right] + \mathcal{O}(|z|^3, |\bar{z}|^3).$$

This is equivalent to

$$W(z, \bar{z}, \rho) = W_{20}(\rho) \frac{z^2}{2} + W_{11}(\rho) z\bar{z} + W_{02}(\rho) \frac{\bar{z}^2}{2} + W_{30}(\rho) \frac{z^3}{6} + \dots \quad (32)$$

where z and \bar{z} are the local coordinates of the center manifold C_0 in the direction of b^* and \bar{b}^* at $\sigma = 0$. We note that the stable manifold W is real if e_t is real and therefore consider the real solutions only. From $e_t \in C_0$ of (28) and (30) at $\sigma = 0$, we have $\dot{z}(t) = \langle b^*, \dot{e}_t \rangle$,

from which (29) yields
$$\dot{z}(t) = \langle b^*, A(0)e_t + N(0)e_t \rangle,$$

and the inner product yields

$$\dot{z}(t) = A(0)\langle b^*, e_t \rangle + \bar{b}^*(0)N_1(W(z, \bar{z}, 0) + 2R_e[z(t)b(0)]).$$

By (31), we have

$$\dot{z}(t) = i\tilde{\omega}\tilde{\tau}\langle b^*, e_t \rangle + \bar{b}^*(0)N_0(z, \bar{z})$$

where,

$$N_0(z, \bar{z}) = N_1(W(z, \bar{z}, 0) + 2R_e[z(t)b(0)]),$$

for $\rho = 0$. Hence, we can define

$$\dot{z}(t) \doteq i\tilde{\omega}\tilde{\tau}z(t) + \bar{b}^*(0)N_0(z, \bar{z}),$$

and re-write equation (31) as

$$\dot{z}(t) = i\tilde{\omega}\tilde{\tau}z(t) + g(z, \bar{z}),$$

where,

$$g(z, \bar{z}) = \bar{b}^*(0)N_0(z, \bar{z}), \text{ and } g_{20} \frac{z^2}{2} + g_{11}z\bar{z} + g_{02} \frac{\bar{z}^2}{2} + g_{21} \frac{z^2\bar{z}}{2} + \dots \quad (33)$$

while using Hopf bifurcation of definition 2. From (31) and (32), we have

$$e_t(\rho) = W(t, \rho) + 2R_e\{z(t)b(\rho)\}, \\ = W(t, \rho) + (z(t)b(\rho) + \bar{z}(t)\bar{b}(\rho)),$$

since $z + \bar{z} = 2R_e$.

Therefore, we can compactly write (31) as

$$e_t(\rho) = W_{20}(\rho) \frac{z^2}{2} + W_{11}(\rho) z\bar{z} + W_{02}(\rho) \frac{\bar{z}^2}{2} + (1, \zeta)^T e^{i\tilde{\omega}\tilde{\tau}\rho} z + (1, \bar{\zeta})^T e^{-i\tilde{\omega}\tilde{\tau}\rho} \bar{z}. \quad (34)$$

This can further be expressed and separate in vector form given by

$$e_1(t + \rho) = W_{20}^{(1)}(\rho) \frac{z^2}{2} + W_{11}^{(1)}(\rho) z\bar{z} + W_{02}^{(1)}(\rho) \frac{\bar{z}^2}{2} + e^{i\tilde{\omega}\tilde{\tau}\rho} z + e^{-i\tilde{\omega}\tilde{\tau}\rho} \bar{z}$$

and

$$e_2(t + \rho) = W_{20}^{(2)}(\rho) \frac{z^2}{2} + W_{11}^{(2)}(\rho) z\bar{z} + W_{02}^{(2)}(\rho) \frac{\bar{z}^2}{2} + \zeta e^{i\tilde{\omega}\tilde{\tau}\rho} z + \bar{\zeta} e^{-i\tilde{\omega}\tilde{\tau}\rho} \bar{z},$$

where,

$$e_t = (e_1(t), e_2(t))^T \in \mathbb{R}_+^2 \quad \text{and} \quad b(\rho) = (1, \zeta)^T e^{i\tilde{\omega}\tilde{\tau}\rho}.$$

From $b^*(s) = \bar{D} \left((1, \bar{\zeta}^*) e^{i\tilde{\omega}\tilde{\tau}s} \right)$, we have from (26) and (33) such that

$$G(z, \bar{z}) = \bar{b}^*(0)N_0(0, e_t) \\ = \tilde{\tau}\bar{D}(1, \bar{\zeta}^*) \begin{pmatrix} -\beta e_{1,t}(0)e_{2,t}(0) \\ \beta e_{1,t}(-1)e_{2,t}(0) \end{pmatrix} \\ = -\tilde{\tau}\beta\bar{D} [e_{1,t}(0)e_{2,t}(0) - \bar{\zeta}^* e_{1,t}(-1)e_{2,t}(0)] \\ = (-\tilde{\tau}\bar{D}\beta A_1)A_2 + (\tilde{\tau}\bar{D}\beta\bar{\zeta}^* A_3)A_4 \quad (35)$$

where

$$A_1 = z + \bar{z} + W_{20}^{(1)}(0) \frac{z^2}{2} + W_{11}^{(1)}(0) z\bar{z} + W_{02}^{(1)}(0) \frac{\bar{z}^2}{2} + W_{30}^{(1)}(0) \frac{z^3}{6} + \dots$$

$$A_2 = \zeta z + \bar{\zeta} \bar{z} + W_{20}^{(2)}(0) \frac{z^2}{2} + W_{11}^{(2)}(0) z\bar{z} + W_{02}^{(2)}(0) \frac{\bar{z}^2}{2} + \dots$$

$$A_3 = ze^{i\tilde{\omega}\tilde{\tau}} + \bar{z}e^{-i\tilde{\omega}\tilde{\tau}} + W_{20}^{(1)}(-1) \frac{z^2}{2} + W_{11}^{(1)}(-1) z\bar{z} + W_{02}^{(1)}(-1) \frac{\bar{z}^2}{2} + \dots$$

$$A_4 = \zeta z + \bar{\zeta} \bar{z} + W_{20}^{(2)}(0) \frac{z^2}{2} + W_{11}^{(2)}(0) z\bar{z} + W_{02}^{(2)}(0) \frac{\bar{z}^2}{2} + \dots$$

Comparing the coefficients with (35), we have

$$g_{20} = -\tilde{\tau}\bar{D}\beta(\zeta - \zeta\bar{\zeta}^* e^{-i\tilde{\omega}\tilde{\tau}}) \\ g_{11} = \tilde{\tau}\bar{D}\beta(Re\{\zeta\} - \bar{\zeta}^* Re\{\zeta\}) \\ g_{02} = -\tilde{\tau}\bar{D}\beta(\bar{\zeta} - \bar{\zeta}\zeta^* e^{i\tilde{\omega}\tilde{\tau}}).$$

$$g_{21} = -\tilde{\tau}\bar{D}\beta\{L_1 + \tilde{\tau}\bar{D}\beta L_2\} \quad (36)$$

where $L_1 =$

$$(2W_{11}^{(1)}(0) + W_{20}^{(1)}(0)) + (2\zeta W_{11}^{(2)}(0) + \zeta W_{20}^{(2)}(0))$$

$$L_2 = 2e^{-i\tilde{\omega}\tilde{\tau}} (W_{11}^{(1)}(-1) + W_{11}^{(2)}(0)) + e^{i\tilde{\omega}\tilde{\tau}} (\bar{\zeta}^* W_{20}^{(1)}(-1) + \zeta W_{20}^{(2)}(0))$$

From $W_{20}(\rho)$ and $W_{11}(\rho)$ in g_{21} , we need to compute C_0 near the origin. Thus from (29) and (31), we have

$$\dot{W} = \dot{e}_t - \dot{z}b - \dot{\bar{z}}\bar{b},$$

were

$$\dot{W} = \begin{cases} AW - 2R_e[\bar{b}^*(0)N_0(z, \bar{z})b(\rho)], \rho \in [-\tau, 0) \\ AW - 2R_e[\bar{b}^*(0)N_0(z, \bar{z})b(\rho)] + N_0, \rho = 0 \end{cases} \quad (37)$$

$$\dot{W} \doteq AW + H(z, \bar{z}, \rho).$$

By Taylors' series expansion,

$$H(z, \bar{z}, \rho) = H_{20}(\rho) \frac{z^2}{2} + H_{11}(\rho) z\bar{z} + H_{02}(\rho) \frac{\bar{z}^2}{2} + \dots \quad (38)$$

From (37) and for $\rho \in [-\tau, 0)$, we have

$$\begin{aligned} & -2\text{Re}\{ \bar{b}^*(0)N_1(z, \bar{z}, 0)b(\rho) \} \\ & = -\{ \bar{b}^*(0)N_1(z, \bar{z}, 0) + b^*(0)\bar{N}_1(z, \bar{z}, 0) \} b(\rho) \\ & = -\bar{b}^*(0)N_0(0, e_t)b(\rho) - b^*(0)\bar{N}_0(0, e_t)\bar{b}(\rho). \end{aligned}$$

But from (33), we recall that

$$g(z, \bar{z}) = \bar{b}^*(0)N_0(0, e_t) \quad \text{and} \quad \bar{g}(z, \bar{z}) = b^*(0)\bar{N}_0(0, e_t).$$

Hence,

$$\begin{aligned} & -2\text{Re}\{ \bar{b}^*(0)N_1(z, \bar{z}, 0)b(\rho) \} \\ & = -g(z, \bar{z})b(\rho) - \bar{g}(z, \bar{z})\bar{b}. \end{aligned}$$

For center manifold C_0 near the origin, we have the following corresponding series

$$\begin{aligned} (A - 2i\tilde{\omega}\tilde{\tau})W_{20}(\rho) + AW_{11}(\rho) + AW_{02}(\rho) \\ = -H_{20}(\rho) - H_{11}(\rho) - H_{02}(\rho) \end{aligned}$$

and by comparing coefficients, (37) yields

$$\left. \begin{aligned} (A - 2i\tilde{\omega}\tilde{\tau})W_{20}(\rho) &= -H_{20}(\rho) \\ AW_{11}(\rho) &= -H_{11}(\rho) \\ (A - 2i\tilde{\omega}\tilde{\tau})W_{02}(\rho) &= -H_{02}(\rho) \end{aligned} \right\} \quad (39)$$

From (36) and the fact that $\rho \in [-\tau, 0)$, then

$$H(z, \bar{z}, \rho) = -g(z, \bar{z})b^*(\rho) - \bar{g}(z, \bar{z})\bar{b}^*(\rho). \quad (40)$$

Comparing the coefficients of (37) with (38), we get

$$H_{20}(\rho) = -g_{20}b(\rho) - \bar{g}_{02}\bar{b}(\rho), \quad (41)$$

and

$$H_{11}(\rho) = -g_{11}b(\rho) - \bar{g}_{11}\bar{b}(\rho) \quad (42)$$

From (39) and (41) and definition of A for

$$AW_{20}(\rho) = 2i\tilde{\omega}\tilde{\tau}W_{20}(\rho), \text{ it follows that}$$

$$W_{20}(\rho) = 2i\tilde{\omega}\tilde{\tau}W_{20}(\rho) + g_{20}b(\rho) + \bar{g}_{02}\bar{b}(\rho),$$

since $\dot{W}_{20}(\rho) = AW_{20}(\rho)$

Note that $b(\rho) = (1, \zeta)^T e^{i\tilde{\omega}\tilde{\tau}\rho}$ from which $b(0) = (1, \zeta)^T$.

From linear differential equation of the form

$$\dot{W}_{20}(\rho) = 2i\tilde{\omega}\tilde{\tau}W_{20}(\rho) + g_{20}b(\rho) + \bar{g}_{02}\bar{b}(\rho)$$

and on solving the first order linear equation analytically, we obtain

$$W_{20}(\rho) = e^{2i\tilde{\omega}\tilde{\tau}\rho} \left(\frac{g_{20}b(0)e^{-i\tilde{\omega}\tilde{\tau}\rho}}{-i\tilde{\omega}\tilde{\tau}} + \frac{\bar{g}_{02}\bar{b}(0)e^{-3i\tilde{\omega}\tilde{\tau}\rho}}{-3i\tilde{\omega}\tilde{\tau}} + E_1 \right).$$

Thus, the rest of the solution which does not lie on the center subspace is given by

$$W_{20}(\rho) = \frac{ig_{20}}{\tilde{\omega}\tilde{\tau}} b(0)e^{i\tilde{\omega}\tilde{\tau}\rho} + \frac{i\bar{g}_{02}}{3\tilde{\omega}\tilde{\tau}} \bar{b}(0)e^{-i\tilde{\omega}\tilde{\tau}\rho} + E_1 e^{2i\tilde{\omega}\tilde{\tau}\rho}, \quad (43)$$

where $E_1 = (E_1^{(1)}, E_1^{(2)})^T \in \mathbb{R}_+^2$ is a constant vector. Similarly, from (39) and (42), we have:

$$AW_{11}(\rho) = g_{11}b(0) + \bar{g}_{11}\bar{b}(0),$$

since $\dot{W}_{11}(\rho) = AW_{11}(\rho)$.

Therefore,

$$\dot{W}_{11}(\rho) = g_{11}b(0)e^{i\tilde{\omega}\tilde{\tau}\rho} + \bar{g}_{11}\bar{b}(0)e^{-i\tilde{\omega}\tilde{\tau}\rho},$$

and on solving the above first order linear equation analytically, we obtain

$$W_{11}(\rho) = \frac{-ig_{11}}{\tilde{\omega}\tilde{\tau}} b(0)e^{i\tilde{\omega}\tilde{\tau}\rho} + \frac{i\bar{g}_{11}}{\tilde{\omega}\tilde{\tau}} \bar{b}(0)e^{-i\tilde{\omega}\tilde{\tau}\rho} + E_2, \quad (44)$$

where,

$$E_2 = (E_2^{(1)}, E_2^{(2)})^T \in \mathbb{R}_+^2 \text{ is a constant vector.}$$

We next seek the appropriate vectors E_1 and E_2 from (43) and (44).

From definition of A and (39), we can obtain

$$\int_{-\tau}^0 d\eta(\rho) W_{20}(\rho) = 2i\tilde{\omega}\tilde{\tau}W_{20}(0) - H_{20}(0) \quad (45)$$

and

$$\int_{-\tau}^0 \eta(\rho) dW_{11}(\rho) = -H_{11}(0) \quad (46)$$

where $\eta(\rho) = \eta(0, \rho)$. By (37) and for $\rho = 0$, we have

$$H_{20}(0) = -g_{20}b(0) - \bar{g}_{02}\bar{b}(0) + 2\tilde{\tau} \begin{pmatrix} -\beta \\ \beta \end{pmatrix} \quad (47)$$

and

$$H_{11}(0) = -g_{11}b(0) - \bar{g}_{11}\bar{b}(0) + 2\tilde{\tau} \begin{pmatrix} -\beta \\ \beta \end{pmatrix}. \quad (48)$$

By substituting (43) and (47) into (45), we have

$$\int_{-\tau}^0 d\eta(\rho) W_{20}(\rho) = 2i\tilde{\omega}\tilde{\tau}W_{20}(0) - H_{20}(0).$$

This gives

$$\begin{aligned} & \int_{-\tau}^0 d\eta(\rho) \left[\frac{ig_{20}b(0)e^{i\tilde{\omega}\tilde{\tau}\rho}}{\tilde{\omega}\tilde{\tau}} + \frac{i\bar{g}_{02}\bar{b}(0)e^{-i\tilde{\omega}\tilde{\tau}\rho}}{3i\tilde{\omega}\tilde{\tau}} + E_1 e^{2i\tilde{\omega}\tilde{\tau}\rho} \right] \\ & = 2i\tilde{\omega}\tilde{\tau} \left[\frac{ig_{20}b(0)}{\tilde{\omega}\tilde{\tau}} + \frac{i\bar{g}_{02}\bar{b}(0)}{3i\tilde{\omega}\tilde{\tau}} + E_1 \right] + g_{20}b(0) \\ & \quad + \bar{g}_{02}\bar{b}(0) - 2\tilde{\tau} \begin{pmatrix} -\beta \\ \beta \end{pmatrix}. \end{aligned}$$

From definition of A when $\sigma = 0$, we have

$$\int_{-\tau}^0 d\eta(\rho) E_1 e^{2i\tilde{\omega}\tilde{\tau}\rho} = 2i\tilde{\omega}\tilde{\tau}E_1 - 2\tilde{\tau} \begin{pmatrix} -\beta \\ \beta \end{pmatrix}.$$

Solving for E_1

$$\left(2i\tilde{\omega}\tilde{\tau}I_2 - \int_{-\tau}^0 d\eta(\rho) e^{2i\tilde{\omega}\tilde{\tau}\rho} \right) E_1 = 2\tilde{\tau} \begin{pmatrix} -\beta \\ \beta \end{pmatrix}, \quad (49)$$

where I_2 is the identity matrix of order 2.

From the definition of A when $\sigma = 0$, we have

$$\int_{-\tau}^0 d\eta(\rho) e^{2i\tilde{\omega}\tilde{\tau}\rho} = \tilde{\tau} \begin{pmatrix} -\frac{\pi\beta}{(\gamma+\mu)} & -(\gamma+\mu) \\ 0 & -(\gamma+\mu) \end{pmatrix} + \tilde{\tau} \begin{pmatrix} 0 & 0 \\ \frac{\pi\beta-\mu(\gamma+\mu)}{(\gamma+\mu)} e^{-2i\tilde{\omega}\tilde{\tau}} & 0 \end{pmatrix}, \rho = 0$$

$$= \tilde{\tau} \begin{pmatrix} -\frac{\pi\beta}{(\gamma+\mu)} & -(\gamma+\mu) \\ \left(\frac{\pi\beta-\mu(\gamma+\mu)}{(\gamma+\mu)}\right) e^{-2i\tilde{\omega}\tilde{\tau}} & -(\gamma+\mu) \end{pmatrix}$$

Therefore, from (49) and the fact that the set of all solutions of the homogeneous equation is a vector of the form:

$$(2i\tilde{\omega}\tilde{\tau}\mathbf{I}_2 - A)b(0) = 2\tilde{\tau} \begin{pmatrix} -\beta \\ \beta \end{pmatrix}, \text{ for } \rho = 0,$$

Thus, equation (49) yields

$$\begin{pmatrix} 2i\tilde{\omega}\tilde{\tau} + \frac{\pi\beta}{(\gamma+\mu)} & (\gamma+\mu) \\ -\frac{\pi\beta-\mu(\gamma+\mu)}{(\gamma+\mu)} e^{-2i\tilde{\omega}\tilde{\tau}} & 2i\tilde{\omega}\tilde{\tau} + (\gamma+\mu) \end{pmatrix} E_1 = 2 \begin{pmatrix} -\beta \\ \beta \end{pmatrix} \quad (50)$$

By Cramer's rule, we have

$$E_1^{(1)} = \frac{2}{A} \begin{vmatrix} -\beta & (\gamma+\mu) \\ \beta & 2i\tilde{\omega}\tilde{\tau} + (\gamma+\mu) \end{vmatrix},$$

and

$$E_1^{(2)} = \frac{2}{A} \begin{vmatrix} 2i\tilde{\omega}\tilde{\tau} + \frac{\pi\beta}{(\gamma+\mu)} & -\beta \\ -\left(\frac{\pi\beta-\mu(\gamma+\mu)}{(\gamma+\mu)}\right) e^{-2i\tilde{\omega}\tilde{\tau}} & \beta \end{vmatrix},$$

$$\text{where } A = \begin{vmatrix} 2i\tilde{\omega}\tilde{\tau} + \frac{\pi\beta}{(\gamma+\mu)} & (\gamma+\mu) \\ -\frac{\pi\beta-\mu(\gamma+\mu)}{(\gamma+\mu)} e^{-2i\tilde{\omega}\tilde{\tau}} & 2i\tilde{\omega}\tilde{\tau} + (\gamma+\mu) \end{vmatrix}.$$

Similarly, by substituting (44) and (48) into (46), we obtain

$$\int_{-\tau}^0 d\eta(\rho) W_{11}(\rho) = -H_{11}(0)$$

from which we have

$$\int_{-\tau}^0 d\eta(\rho) \left[-\frac{i\bar{g}_{11}}{\tilde{\omega}\tilde{\tau}} b(0) e^{i\tilde{\omega}\tilde{\tau}\rho} + \frac{i\bar{g}_{11}}{\tilde{\omega}\tilde{\tau}} \bar{b}(0) e^{-i\tilde{\omega}\tilde{\tau}\rho} + E_2 \right] = g_{11} b(0) + \bar{g}_{11} \bar{b}(0) - 2\tilde{\tau} \begin{pmatrix} -\beta \\ \beta \end{pmatrix}.$$

From the definition of A when $\sigma = 0$, E_2 yields

$$\int_{-\tau}^0 d\eta(\rho) E_2 = -2 \begin{pmatrix} -\beta \\ \beta \end{pmatrix} \quad (51)$$

where

$$E_2 = (E_2^{(1)}, E_2^{(2)})^T \in \mathbb{R}_+^2 \text{ is a constant vector.}$$

From (50) and the fact that the set of all solutions of the homogeneous equation is a vector, we have

$$\begin{pmatrix} \frac{\pi\beta}{(\gamma+\mu)} & (\gamma+\mu) \\ \frac{\pi\beta-\mu(\gamma+\mu)}{(\gamma+\mu)} & (\gamma+\mu) \end{pmatrix} E_2 = -2 \begin{pmatrix} -\beta \\ \beta \end{pmatrix}. \quad (52)$$

By Cramer's rule, (52) yields

$$E_2^{(1)} = \frac{2}{B} \begin{pmatrix} \beta & (\gamma+\mu) \\ -\beta & (\gamma+\mu) \end{pmatrix}$$

and

$$E_2^{(2)} = \frac{2}{B} \begin{pmatrix} \frac{\pi\beta}{(\gamma+\mu)} & \beta \\ \frac{\pi\beta-\mu(\gamma+\mu)}{(\gamma+\mu)} & -\beta \end{pmatrix},$$

where

$$B = \begin{vmatrix} \frac{\pi\beta}{(\gamma+\mu)} & (\gamma+\mu) \\ \frac{\pi\beta-\mu(\gamma+\mu)}{(\gamma+\mu)} & (\gamma+\mu) \end{vmatrix}.$$

Note that from (43), (44), (50) and (52), g_{21} of (36) can be approximated by given specific values of parameters and delay term. We thus compute $W_{20}(\rho)$ and $W_{11}(\rho)$ from (43) and (44) as well. We can then compute the values:

$$C_1(0) = \frac{i}{2\tilde{\omega}\tilde{\tau}} (g_{20}g_{11} - 2|g_{11}|^2 - \frac{|g_{02}|^2}{3}) + \frac{g_{21}}{2} \quad (53)$$

Define

$$\mu_2 = -\frac{Re\{C_1(0)\}}{Re\left\{\frac{d}{d\tau}\lambda(\tilde{\tau})\right\}},$$

$$\beta_2 = 2Re\{C_1(0)\},$$

$$T_2 = -\frac{Im\{C_1(0)\} + \mu_2 Im\left\{\frac{d\lambda(\tilde{\tau})}{d\tau}\right\}}{\tilde{\omega}\tilde{\tau}}.$$

Then, the general results describe the properties of the periodic solutions where the center manifolds of (3) splits at the value $\tilde{\tau}$ for $Re\left(\frac{d\lambda(\tilde{\tau})}{d\tau}\right) > 0$ such that:

1. μ_2 determines the direction of Hopf bifurcation where the solutions in center manifold of (3) splits. If $\mu_2 > 0$, supercritical splitting occurs and if $\mu_2 < 0$, subcritical splitting occurs. Thus, bifurcating periodic solutions occurs for $\tau > \tilde{\tau}$ (supercritical) or $\tau < \tilde{\tau}$ (subcritical).
2. β_2 determines the stability of the bifurcating periodic solutions such that for $\beta_2 < 0$, stability occurs and unstable for $\beta_2 > 0$.
3. T_2 determines the period of the bifurcating periodic solutions such that if $T_2 > 0$, the period increases, and decreases if $T_2 < 0$.

4.2 Numerical Simulations

Since Systems (2) and (3) have properties that make their solutions complicated to solve using explicit methods, there is the need for numerical techniques to investigate the behavior of their solutions. Figure 3, Figure 4, Figure 5, Figure 6, Figure 7, Figure 8, Figure 9, Figure 10, Figure 11, Figure 12, Figure 13,

Figure 14 and Figure 15 showed numerical results of (2) and (3) at different values of delay parameters when $\beta = 0.31, \gamma = 0.6, \mu = 0.1$ and $\alpha = 0.11$ as in the works of previous authors. From the parameter values, the calculated crossing frequency $\omega_0 \in \mathbb{R}_+ = 0.5972$ and the threshold delay margin $\tau_c = 1.9510$. Periodic solutions exist since closed curve splits and Hopf bifurcation occurs as seen in Figure 3, Figure 4, Figure 5, Figure 6, Figure 7, Figure 8, Figure 9, Figure 10, Figure 11, Figure 12, Figure 13, Figure 14 and Figure 15.

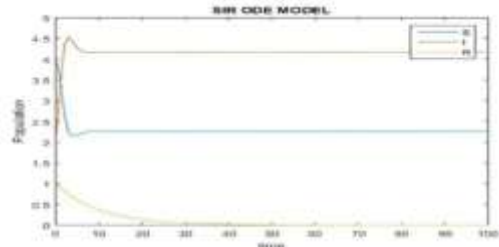


Fig. 3: Asymptotic Stability of Model 2
 At $\tau = 0$, the model (1) is asymptotically stable.

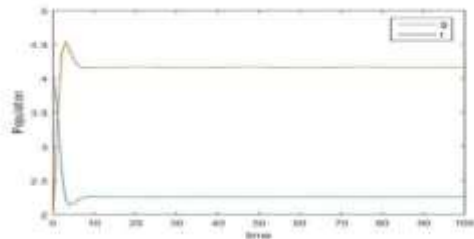


Fig. 4: Asymptotic Stability of Model 3
 For $\tau = 0$, the model (3) is asymptotically stable.

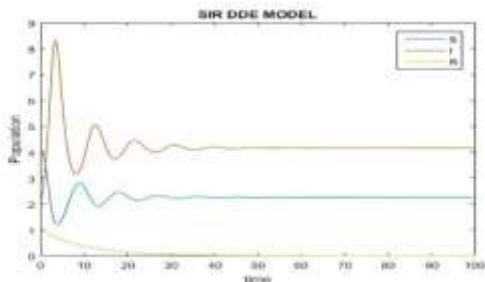


Fig. 5: Asymptotic Stability of Model 2
 For $\tau = 1.5 < \tau_c = 1.9510$, the model (2) is asymptotically stable.

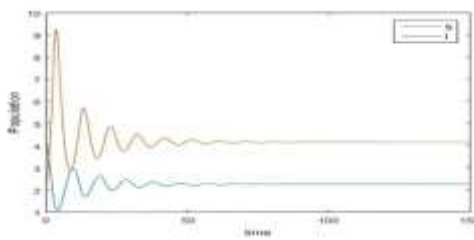


Fig. 6: Asymptotic Stability of Model 3

For $\tau = 1.5 < \tau_c = 1.9510$, the model (3) is asymptotically stable.

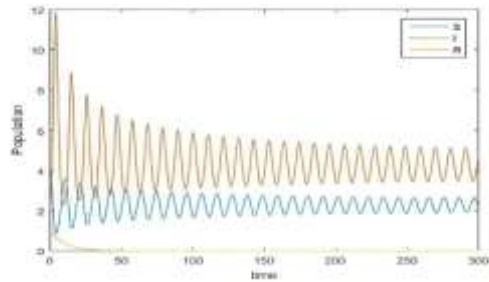


Fig. 7: Periodic Solutions of Model (2)
 At $\tau = \tau_c = 1.9510$, the periodic solutions of (2) occur.

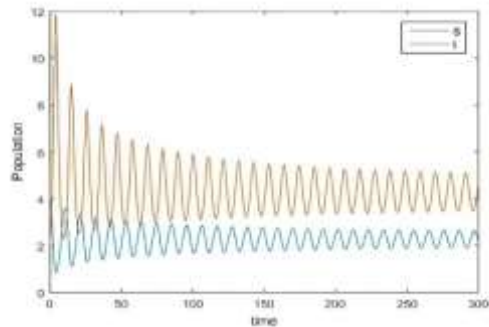


Fig. 8: Periodic Solutions of Model (3)
 At $\tau = \tau_c = 1.9510$, the periodic solutions of (3) occur.

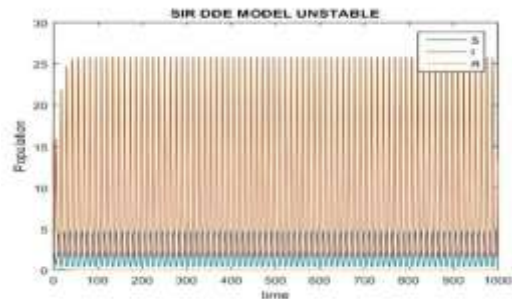


Fig. 9: Chaotic Solutions of Model (2)
 At $\tau = 2.5 > 1.9510$, chaotic solutions of (2) occur.

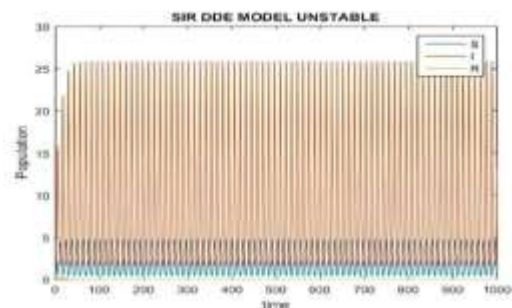


Fig. 10: Aperiodic Solutions of Model (3)
 For $\tau = 2.5 > 1.9510$ Aperiodic solutions of (3) occur.

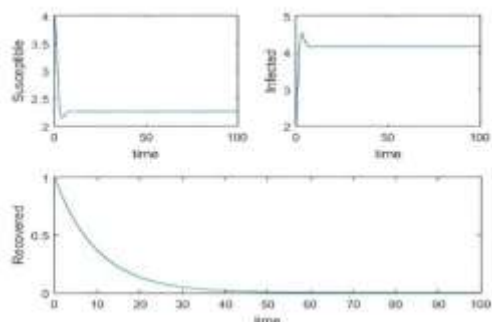


Fig. 11: Aperiodic Solutions of Model (2)
 For $\tau = 2.5 > \tau_c = 1.9510$. Aperiodic Solutions of (2) occur.

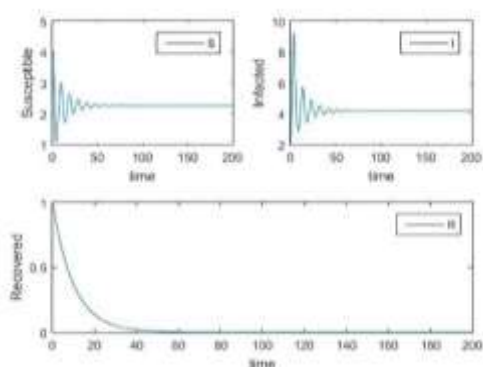


Fig. 12: Asymptotic Stability of Model (2)
 For $\tau = 1.5 < \tau_c = 1.9510$, the model (2) is asymptotically stable.

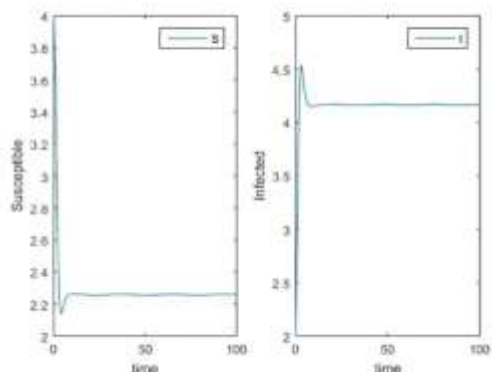


Fig. 13: Asymptotic Stability of Model (3)
 For $\tau = 1.5 < \tau_c = 1.9510$, the trivial solution of (3) is asymptotically stable.

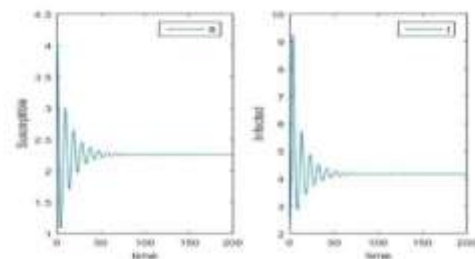


Fig. 14: Asymptotic Stability of Model (3)

For $\tau = 1.5 < \tau_c = 1.9510$, the endemic solution of (3) is asymptotically stable as seen from above.

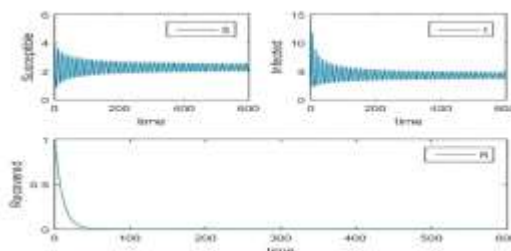


Fig. 15: Periodic Stability of Model (2)
 If $\tau = 2.5 > 1.9510$, the solution of (2) becomes chaotic

5 Numerical Applications

5.1 Numerical Example and Discussion

The numerical example yields the plots in Figure 3, Figure 4, Figure 5, Figure 6, Figure 7, Figure 8, Figure 9, Figure 10, Figure 11, Figure 12, Figure 13, Figure 14 and Figure 15. The susceptible population reduces to a lower level due to the aftermath of the disease transmission rate. This reduction in population gradually decreases as the infection rate increases as can be seen in Figure 3, Figure 4, Figure 5, Figure 6, Figure 7, Figure 8, Figure 9, Figure 10, Figure 11, Figure 12, Figure 13, Figure 14 and Figure 15. However, at $\tau = 0$, (2) becomes (1) and are asymptotically stable (Figure 3 and Figure 4). It is observed from the presence of periodic solutions that the closed curve splits. Despite the introduction of threshold value R_0 of (2) and (3), the result of the analysis showed that the DFE and endemic equilibrium points cannot coexist simultaneously. From the characteristic polynomial of the DFE, the eigenvalues at $R_0 < 1$ of (2) and (3) become locally asymptotically stable (LAS). This result supports the Routh-Hurwitz criterion. Also, for $R_0 < 1$ the disease dies out while for $R_0 > 1$ the infection is maintained, and the disease becomes endemic in the population. For $\tau = 1.5 < \tau_c = 1.9510$, (2) and (3) are locally asymptotically stable (Figure 5 and Figure 6). At $\tau = \tau_c = 1.9510$, the closed curve splits and the existence of periodic solutions are guaranteed (Figure 7 and Figure 8). If $\tau = 2.5 > \tau_c = 1.9510$, the solutions of (2) and (3) become chaotic (Figure 9 and Figure 10).

The consequence of time delay on the dynamical properties of (3) were further examined when the Hartman-Grobman's theorem is not satisfied. *i.e.*, when $R_0 = 1$. Further conditions of stability and Hopf bifurcation analyses of model (3) were derived and used to investigate more general

properties and behavior of stability of the SIR system. As in the study, these conditions are sufficient but not necessary as delay models were unable to stabilize the unstable positive equilibrium. In addition, the study determined conditions for Hopf bifurcation for stability analysis of positive equilibrium of the reduced model and provides realistic explicit algorithm for investigating the direction and further stability properties of (3) using the normal form concept (NFC) and CMT of the associated operator differential equation (OpDE) when the linearized form of the system has at least one characteristic root with zero real part while every other eigenvalues have negative real parts. Although, the analysis of DDE of (3) displays very robust dynamics arising from analytical analysis of the solution. This paper is suitable for large population densities.

5.2 Concluding Remarks

The SIR delay disease model successfully determined many parameters for stability analysis. The dynamics of infection diseases and spreading patterns were dependent on the basic threshold value R_0 . The control of infectious disease models also depends on the threshold value R_0 . The endemic equilibrium exists when the infection rate is greater than the deaths, *i.e.* when $R_0 > 1$. Although, the underlying delay differential equation (DDE) model provided a formal structure of stability analysis when $R_0 = 1$ and make analytical investigations of delay models possible for wider range of applications.

5.3 Applications

The SIR mathematical epidemic disease delay model considered in this study is very useful for controlling the dynamics of infectious diseases in a given population. It applies basic indices of infectious diseases dynamics to important parameters in determining stability properties of (2) and (3). The generalized reduced disease model is realistic for investigating stability and Hopf bifurcation analyses in epidemiology and other related models of lower dimension. In addition, the study provided an interesting formal structure for stability analyses to specialists in biomathematics, ecology, biology and public health workers, for decision making purposes.

References:

[1] Edessa, G. K., and Koya, P. R. (2020). Modelling and stability analysis of a three species ecosystem with the third species

response to the first species in sigmoid functional response form. *Mathematical Modelling and Applications*, Vol.5 No.3, pp. 156-166. doi: 10.11648/j.mma.20200503.14.

- [2] Getto, P., Gyllenberg, M., Nakata, Y., and Scarabel, F. (2019). Stability analysis of a state dependent delay differential equation for cell maturation: analytical and numerical methods. *Journal of Mathematical Biology*, Vol.79 No.1, pp. 281–328. doi:10.1007/s00285-019-01357-0.
- [3] Chena, D. W., Xua, Z., Leia, Z., Huang, J., Liua, B., Gaoa, Z. and Penga, L. (2020). Recurrence of positive SARS-CoV-2 RNA in COVID - 19: A case report. *International Journal of infectious Diseases*, Vol.93, pp. 297-299.
- [4] Naveed, M, Baleanu, D., Rafiq, M., Raza, A., Soori, H., and Ahmed, A. (2020). Dynamical behavior and sensitivity analysis of a delayed corona virus epidemic model. *Computers, Materials and Continua*, Vol.65 No.1, pp. 225–241. doi: 10.32604/cmc.2020.011534.
- [5] Glass, D. S., Jin, X., and Riedel-Kruse, I. H. (2021). Nonlinear delay differential equations and their application to modelling biological network motifs. *Nature Communication*, Vol.12, pp. 1788. doi:10.1038/s41467-021-21700-8.
- [6] Dumbela, P. A., and Aldila, D. (2019). Dynamical analysis in Predator-Prey scavenger model with harvesting intervention on prey population. *AIP Conference Proceedings* 2192, 060005. doi:10.1063/1.5139151.s.
- [7] Jayanthan, R., and Krishnan, M. (2022). Stability analysis of delayed SIR model with logistic growth and bilinear incidence rate. *Journal of mathematical and Computational Science*, 12 Article ID 124. doi:10.28919/jmcs/7275.
- [8] Edeki, S. O., Adinya, I., Adeosun, M. E., and Ezekiel, I. D. (2020). Mathematical analysis of the global COVID-19 spread in Nigeria and Spain based on SEIR model. *Communications in Mathematical Biology and Neuroscience*, Article ID 84.
- [9] Ezekiel, I. D, Iyase, S. A. and Anake, T. A. (2022). Stability Analysis of an SIR Infectious Disease Model, *ICORTAR Journal of Physics: Conference Series* 2199 012035 IOP Publishing doi: 10.1088/1742-6596/2199/1/012035.
- [10] Tang, B., Bragazzi, N. L., Tang, Q., Li, S., Xiao, Y., and Wu, J. (2020). An updated

- estimation of the risk of transmission of the novel corona virus (2019-nCov). *Infectious Disease Modelling*, 5 (2020), pp. 248–255. doi: 10.1016/j.idm.2020.02.001.
- [11] Riou J. and Althaus, C. L. (2020). Pattern of early human-to-human transmission of Wuhan 2019 novel corona virus (2019-nCoV), December 2019 to January 2020. *Euro Surveillance*, Vol.25 No.4: 2000058. doi: 10.2807/1560-7917.ES.2020.25.4.2000058.
- [12] van den Driessche P., (2017): Reproduction numbers of infectious disease models. *Infectious Disease Modelling* (2017), Volume 2, Issue 3, pp. 288-303, doi: 10.1016/j.idm.2017.06.002.
- [13] Tipsri, S., and Chinviriyasit, W. (2014). Stability analysis of SEIR model with saturated incidence and time delay. *International Journal of Applied Physics and Mathematics*, Vol.4, pp. 42–45. doi: 10.7763/IJAPM.2014.V4.252.
- [14] Kermack, W. O., and McKendrick, A. G. (1927). A Contribution to the mathematical Theory of Epidemics. *Proceedings of the Royal Society of London. Series A, Containing Papers of a Mathematical and Physical Character* 115(772), 700–721. doi: 10.1098/rspa.1927.0118.
- [15] Tuite, A. R., and Fisman, D. N. (2019). Reporting, epidemic growth, and reproduction numbers for the 2019 novel Corona virus epidemic. *Annals of Internal Medicine*, Vol. 172, Number 8, <https://doi.org/10.7326/m20-0358>.
- [16] Mizumoto, K., and Chowell, G. (2020). Transmission potential of the novel corona virus (COVID-19) on board the diamond Princess Cruises Ship, *Infectious Disease Modelling*, Vol.5, pp. 264 –270. doi:10.1016/j.idm.2020.02.003.
- [17] Zhang, L., Mao, Z., Niculescu S., and Cela, A. (2019). Stability analysis for a class of distributed delay system with a constant coefficient by applying frequency-sweeping approach. *IET Control Theory and Applications*. Vol.13 No.1, pp. 87- 95.
- [18] Hethcote, H. W. (2000). The mathematics of infectious diseases. *Society for Industrial and Applied Mathematics*, SIAM Review, Vol. 42, Issue 4, (2000), <https://doi.org/10.1137/S0036144500371907>.
- [19] Satar, H. A., and Najj, R. K. (2019). Stability and bifurcation of a prey predator-scavenger model in the existence of toxicant and harvesting, *International Journal of Mathematics and Mathematical Sciences*, Article ID 1573516. doi:10.1155/2019/1573516.
- [20] Majid, B. (2017). Analysis and Application of Delay Differential Equations in Biology and Medicine. *Dynamical systems in biology*, 1(25). <https://doi.org/10.48550/arXiv.1701.04173>.
- [21] Arya, N., Bhatia, S. K., and Kumar, A. (2021). Stability and bifurcation analysis of a contaminated SIR model with saturated type incidence rate and Holling type-III Treatment function. *Communications in Mathematical Biology and Neuroscience*, Article ID 3. <https://doi.org/10.28919/cmbn/6887>.
- [22] Nuaimi, A. M., and Jawad, S. (2022). Modelling and Stability analysis of the computational ecological mode with harvesting. *Communications in Mathematical Biology and Neuroscience*, Article ID 47. doi: 10.28919/7450.
- [23] Sudipa Chaochan, Om Prakash Misra, and Joydip Phar (2014). Stability Analysis of SIR Model with vaccination. *American Journal of Computational and Applied Mathematics*. Vol.4 No.1, pp. 17-23.
- [24] Bellman, R., and Cooke, K. L. (1963). *Differential Difference Equations*. New-York: Academic Press.
- [25] Nia, M. F., and Rezaei, F. (2019). Hartman-Grobman's theorem for iterated function systems, *Rocky Mountain Journal of Mathematics*, Vol.49, pp. 307-333. doi:10.1216/RMJ-2019-49-1-307.
- [26] De-Jesus, L. F., Silva, C. M., and Vilarinho, H. (2020). Periodic orbits for periodic eco-epidemiological systems with infected prey. *Electronic Journal of Qualitative Theory of Differential Equations*, Vol.54, pp. 1–20.
- [27] Song, P., and Xiao, Y. (2018). Global Hopf bifurcation of a delayed equation describing the lag effect of media impact on the spread of infectious disease. *Journal of Mathematical Biology*, Vol.76, pp. 1249–1267. doi: 10.1007/s00285-017-1173-y.
- [28] Yang, X., Chen, L., and Chen, J. (1996). Permanence and positive periodic solution for the single species non-autonomous delay diffusive models, *Computational Mathematics Applications*, Vol.32, pp. 9–116. [https://doi.org/10.1016/0898-1221\(96\)00129-0](https://doi.org/10.1016/0898-1221(96)00129-0).
- [29] Smith, H. (2011). An introduction to delay differential equations with applications to the life sciences. New York: Springer-Verlag.

- [30] Sastry, S. (1999). *Nonlinear Systems: Analysis, Stability and Control*. Springer-Verlag, New-York.
- [31] Castillo-Chavez, C., and Song, B. (2004). Dynamical models of tuberculosis and their applications, *Mathematical Biosciences and Engineering*, Vol.2 No.1, pp. 361–404. doi: 10.3934/mbe.2004.1.361.
- [32] Kamrujjaman, M., Lima, S. A., Akter, S., and Eva, T. (2019). Stability Analysis and Numerical solutions of a competition model with the effects of distribution parameters. *Journal of Bangladesh Academy of Sciences*, Vol.43 No.1, pp. 95 -106. <https://doi.org/10.3329/jbas.v43i1.42238>.
- [33] Hassard, B. D., Kazarinoff, N. D., and Wan, Y. H. (1981). *Theory and Application of Hopf Bifurcation*, Cambridge University, Cambridge.
- [34] Hale, J. K. (1977). *Theory of Functional Differential Equations*, Springer-Verlag, New York.

Contribution of Individual Authors to the Creation of a Scientific Article (Ghostwriting Policy)

The authors equally contributed to the present research, at all stages from the formulation of the problem to the final findings and solution.

Sources of Funding for Research Presented in a Scientific Article or Scientific Article Itself

Covenant University Centre for Research, Innovation and Discovery.

Conflict of Interest

The authors have no conflicts of interest to declare.

Creative Commons Attribution License 4.0 (Attribution 4.0 International, CC BY 4.0)

This article is published under the terms of the Creative Commons Attribution License 4.0

<https://creativecommons.org/licenses/by/4.0/deed.en>
[US](https://creativecommons.org/licenses/by/4.0/deed.en)